Supporting Information for

Homochiral Columns Constructed by Chiral Self-Sorting During Supramolecular Helical Organization of Hat-Shaped Molecules

Cécile Roche,[†] Hao-Jan Sun, [†,‡] Margaret E. Prendergast,[†] Pawaret Leowanawat,[†] Benjamin E. Partridge,[†] Paul A. Heiney,[‡] Fumito Araoka,[≠] Robert Graf,[§] Hans W. Spiess,[§] Xianbing Zeng,[¶] Goran Ungar,[¶,♣] and Virgil Percec*,[†]

[†]Roy & Diana Vagelos Laboratories, Department of Chemistry, University of Pennsylvania, Philadelphia, Pennsylvania 19104-6323, United States. [‡]Department of Physics and Astronomy, University of Pennsylvania, Philadelphia, Pennsylvania 19104-6396, United States. [≠]RIKEN Center for Emergent Matter Science, 2-1 Hirosawa, Wako, Saitama 351-0198, Japan. [§]Max-Planck Institute for Polymer Research, 55128 Mainz, Germany. [¶]Department of Materials Science and Engineering, University of Sheffield, Sheffield S1 3JD, United Kingdom. [♣]Department of Physics, Zhejiang Sci-Tech University, Hangzhou 310018, China.

* E-mail: percec@sas.upenn.edu

Table of Contents

1. Materials

3,4-Dihydroxybenzoic acid (98%) (Acros), 3,4-dimethoxybenzyl alcohol (96%), (S)-(+)-citronellylbromide (95%), (R)-(-)-citronellylbromide (95%), thionyl chloride (99.5%), $LiAlH_4$ (95%), boron tribromide, anhydrous K_2CO_3, aluminum oxide (activated, basic, Brockmann I, standard grade, ~150 mesh, 58 Å) (all from Aldrich), methanol, ethanol, acetone, *N*,*N*-dimethylformamide, diethyl ether, ethyl acetate, H_3PO_4 (85%), $NaHCO_3$, Na_2SO_4, $MgSO_4$, KOH, HCl (all from Fisher, ACS reagents), and silica gel (60 Å, 32-63 μm) (Sorbent Technology) were used as received. Methyl 3,4-dihydroxybenzoate was prepared from the corresponding acid by Fisher esterification with MeOH. Tetrahydrofuran (Fisher, ACS reagent grade) was refluxed over sodium/benzophenone and freshly distilled before use. Dichloromethane (Fisher, ACS reagent grade) was refluxed over CaH_2 and freshly distilled before use. All other chemicals were commercially available and were used as received.

2. Techniques

Solution NMR

^{1}H NMR (500 MHz) and ^{13}C NMR (125 MHz) spectra were recorded on a Bruker DRX 500 instrument. The purity of the products was determined by a combination of thin-layer chromatography (TLC) on silica gel coated aluminum plates (with F_{254} indicator; layer thickness, 200 μm; particle size, 2-25 μm; pore size 60Å, SIGMA-Aldrich) and high pressure liquid chromatography (HPLC) using THF as mobile phase at 1 mL/min, on a Shimadzu LC-10AT high pressure liquid chromatograph equipped with a Perkin Elmer LC-100 oven (40 ℃), containing two Perkin-Elmer PL gel columns of 5 x 10^2 and 1 x 10^4 Å, a Shimadzu SPD-10A UV detector (λ = 254 nm), a Shimadzu RID-10A RI-detector, and a PE Nelson Analytical 900 Series integrator data station.

Differential Scanning Calorimetry (DSC)

Thermal transitions were determined on a TA Instruments Q100 differential scanning calorimeter (DSC) equipped with a refrigerated cooling system with 10 °C min^{-1} heating and cooling rates. Indium was used as calibration standard. The transition temperatures were calculated as the maxima and minima of their endothermic and exothermic peaks. An Olympus BX51 optical microscope (100 X magnifications) equipped with a Mettler FP82HT hot stage and a Mettler Toledo FP90 Central Processor was used to verify thermal transitions and to characterize anisotropic textures.

Density Measurements

A small amount of sample (~ 0.5 mg) were placed in a vial filled with water followed by ultrasonication to remove the air bubbles embedded within the sample. The sample was then sunken to the bottom of the vial due to its higher density compared with water. Potassium iodide (KI) was then added into the solution at ~ 0.1 g per aliquot to gradually increase the solution density. KI was added at an interval of at least 20 min to ensure equilibrium within the solution was reached. When the sample was suspended in the middle of the solution, the density of the sample was identical to that of the solution which is easy to be measured by a volumetric flask.

Matrix-Assisted Laser Desorption/Ionization Time of Flight (MALDI-TOF)

MALDI-TOF mass spectrometry was performed on a PerSeptive Biosystems-Voyager-DE (Framingham, MA) mass spectrometer equipped with a nitrogen laser (337 μm) and operating in linear mode. Internal calibration was performed using Angiotensin II and Bombesin as standards. The analytical sample was obtained by mixing the THF solution of the sample (5-10mg/ml) and THF solution of the matrix (3,5-dimethoxy-4-hydroxy-*trans*-cinnamic acid or 4-hydroxybenzylidenemalononitrile, 10mg/mL) in a 1/5 v/v ratio. The prepared solution of the sample and the matrix (0.5 μL) was loaded on the MALDI-TOF plate and allowed to dry at 23 °C before the plate was inserted into the vacuum chamber of the MALDI-TOF instrument. The laser steps and voltages applied were adjusted depending on both the molecular weight and the nature of each analyzed compound.

Solution Circular Dichroism (CD) Measurements

Circular dichroism (CD) and UV spectroscopy measurements were carried out in a Jasco J-720 Spectropolarimeter. The temperature was controlled by Peltier temperature controller (Jasco PTC-423) or with a Thermo Neslab RTE-111 refrigerated circulator digital temperature controller. Dodecane (99%, Acros) or 1-butanol (99.5%, spectrophotometric grade, Aldrich) were used as solvents.

Micro-spot CD Measurements

The micro-spot CD measurements were performed with a J-720WI CD spectrometer (with ORD option, JASCO Corp.). It equipped with a focal reducing optics included a pair of reflective objective lenses in order to reduce undesirable optical aberration and give wider measurement range from the short near-UV to Vis wavelength. The function of the first lens is for focusing, and the outcoming light is

collected by the second lens. Ultrathin LC cells with thickness less than 1 μm of fused-silica substrates were used to obtain the correct spectral shape. The absorbance at the target optical region was measured to be < 2 optical density (OD) to avoid the saturation effect created by strong absorption of the bulk material. During the measurements, the CD spectra were collected by rotating the cell about the surface normal to avoid the influence of birefringence on CD signals. A pinhole mask was used for sample positioning. The pinhole mask was made of a black paper sheet with a small pinhole and it was placed on the LC cell. The masked sample cell was put in the beam path of the CD spectrometer and it is settled on an XY translation stage. In the present case, the pinhole size is larger than the target domain and the CD signal is weak, so several sample positions were tested in order to give the maximum CD signal intensity. The CD spectra were collected using a single scan with a scan rate of 100 nm/min.

X-ray Diffraction (XRD)

X-ray diffraction (XRD) measurements were performed using Cu-$K_{\alpha 1}$ radiation (λ=1.542 Å) from a Bruker-Nonius FR-591 rotating anode X-ray source equipped with a 0.2 x 0.2 mm^2 filament and operated at 3.4 kW. Osmic Max-Flux optics and triple pinhole collimation were used to obtain a highly collimated beam with a 0.3 x 0.3 mm^2 spot on a Bruker-AXS Hi-Star multiwire area detector. To minimize attenuation and background scattering, an integral vacuum was maintained along the length of the flight tube and within the sample chamber. Samples were held in quartz capillaries (0.7 – 1.0 mm in diameter), mounted in a temperature-controlled oven (temperature precision: ±0.1 ℃, temperature range from -120 ℃ to 270 ℃). The distance between the sample and the detector was 12.0 cm for wide angle diffraction experiments and 54.0 cm for intermediate angle diffraction experiments respectively. Aligned samples for fiber XRD experiments were prepared using a custom made extrusion device.[1] The powdered sample (~10 mg) was heated inside the extrusion device above isotropization temperature. After slow cooling from the isotropic phase, the fiber was extruded in the liquid crystal phase and cooled to 23 ℃. Typically, the aligned samples have a thickness of ~ 0.3-0.7 mm and a length of ~ 3-7 mm. All XRD measurements were done with the aligned sample axis perpendicular to the beam direction. Primary XRD analysis was performed using Datasqueeze Software (version 2.2). Molecular modeling calculations were done using the Materials Studio Modeling version 3.1 software from Accelrys. The package Discover module was used to perform the energy minimizations on the supramolecular structures with the following settings: PCFF or COMPASS force fields and Fletcher-Reeves algorithm for the conjugate gradient method. Cerius2 package (version 4.8.1) was used for fiber XRD simulations.

For the XRD experiments on annealed samples, fiber sample after first cooling from 80 ℃ to 20 ℃ in the XRD chamber was placed inside a thin glass capillary and the capillary was placed in the chamber of a hot stage (Mettler Toledo FP82HT). Then the sample was heated to the desired annealing temperature (60 ℃ or 40 ℃) from room temperature with a rate of 10 ℃/min and annealed at the constant temperature

for 2 h (60 ℃) or 24 h (40 ℃). After annealing, the capillary was cooled down in the hot stage to 20 ℃ with a rate of 10 ℃/min before moving to the XRD chamber for pattern collection.

Solid State NMR

Variable temperature $^{13}C\{1H\}$ CP-MAS NMR spectra recorded with a Bruker Avance III console operating at 700.21 MHz ^{1}H Larmor frequency (176.1 MHz ^{13}C Larmor frequency) using a commercial double resonance probe supporting zirconia rotors with 2.5mm outer diameter. The measurements have been performed at 25 kHz MAS spinning frequency, with 100 kHz rf nutation frequency on both, the ^{1}H and the ^{13}C channel, as well as for ^{1}H heteronuclear decoupling during acquisition using the SPINAL64 scheme. The given temperatures have been corrected for known deviations due to frictional heating under fast spinning conditions based on the temperature dependent chemical shift of lead nitrate. In order to compare the temperature dependence of the CP-MAS signal intensities, spectra with 5120 transients and identical experimental parameters have been recorded in the temperature range from 40 – 100 ℃.

3. Synthesis

2,3,7,8,12,13-Hexamethoxy-10,15-dihydro-5*H*-tribenzo-[*a*,*d*,*g*]cyclononene or cyclotriveratrylene (CTV, **16**) was synthesized according to a modified literature procedure.[2] (*S*)-1-Bromo-3,7-dimethyloctane, (*R*)-1-bromo3,7-dimethyloctane and *rac*-1-bromo3,7-dimethyloctane were synthesized by a procedure reported by Swager et al.[3] The synthesis and characterization of the dendronized CTV *(S)*-**(3,4)dm8*G1-CTV** (**13**) and **(3,4)12G1-CTV** (**17**), and their intermediates (compounds **1**, **5**, **6**, and **10**) were described previously,[4] as well as the synthesis of intermediate **(3,4)8G1-CH$_2$Cl** (**9**).[5]

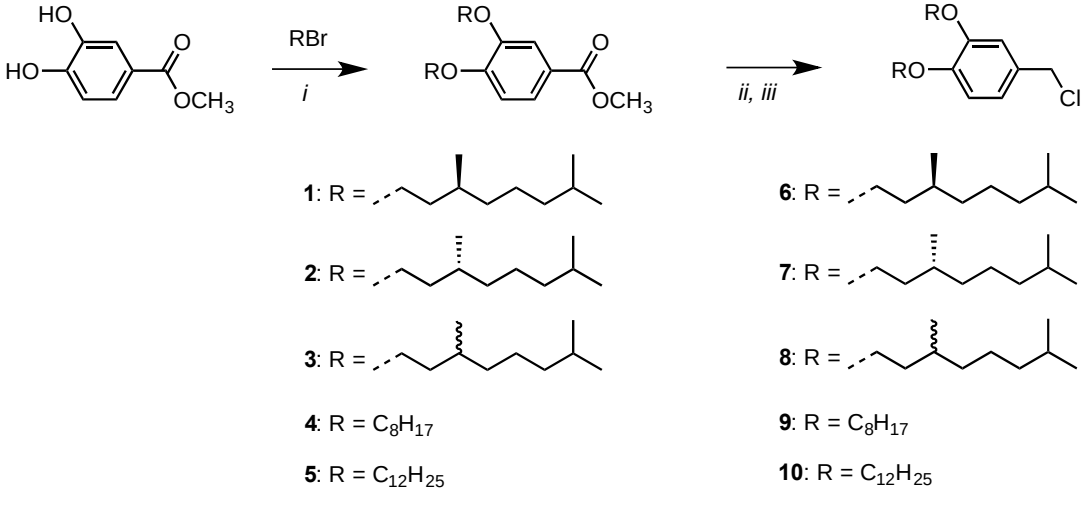

Supporting Scheme SS1. Synthesis of dendrons **6**-**10**. Reagents and condition: *(i)* K_2CO_3, DMF, 70 ℃, 4 h; *(ii)* $LiAlH_4$, THF, 0-23 ℃, 2 h; *(iii)* $SOCl_2$, DMF (cat), 0-23 ℃, 30 min.

***(S)*-(3,4)dm8*G1-CO_2CH_3 (1).** Methyl 3,4-dihydroxybenzoate (1.68 g, 0.01 mol) was added to a degassed suspension of K_2CO_3 (5.53 g, 0.04 mol) in DMF (40 mL) and the mixture was heated to 70 ℃ after which was added (*S*)-3,7-dimethyloctyl bromide (4.45 g, 0.02 mol) and the reaction allowed to stir for 8 h at 70 ℃ under nitrogen. The reaction mixture was cooled to room temperature and poured into cold water. The product was extracted with ether (4x), washed with H_2O (1x) and brine (1x), then dried over anhydrous $MgSO_4$ and concentrated. The crude product was purified by flash column chromatography (basic alumina) using CH_2Cl_2 as eluent to give **1** as colorless viscous liquid (4.05 g, 90%). HPLC: 99+%; TLC (EtOAc/hexane = 1/9): R_f = 0.45; ^{1}H NMR (500 MHz, $CDCl_3$, 27 ℃, TMS): δ = 7.65 (dd, 1H, *J* = 6.5, 2.0 Hz), 7.54 (s, 1H), 6.88 (d, 1H, *J* = 8.5 Hz), 4.09-4.04 (m, 4H), 3.88 (s, 3H), 1.87-1.80 (m, 2H), 1.63 (m, 4H), 1.47 (m, 2H), 1.33-1.31 (m, 6H), 1.17-1.14 (m, 6H), 0.94 (d, 6H, *J* = 6.5 Hz), 0.87 (d, 12H, *J* = 6.6 Hz); ^{13}C NMR (125 MHz, 27 ℃, $CDCl_3$): δ = 167.2, 153.3, 148.7, 123.7, 122.5, 114.1, 111.9, 67.7, 67.5, 53.6, 39.6, 37.5, 36.3, 30.1, 28.3, 24.9, 22.9, 22.8, 19.9 ppm.

***(R)*-(3,4)dm8*G1-CO_2CH_3 (2).** This compound was synthesized by the same procedure described for the synthesis of compound **1**. From methyl 3,4-dihydroxybenzoate (1.18 g, 0.007 mol), K_2CO_3 (3.87 g, 0.028 mol) and (*R*)-1-bromo-3,7-dimethyloctane (3.10 g, 0.014 mol) in DMF (30 mL), compound **2** (2.88 g, 88%) was obtained as colorless viscous liquid. HPLC: 99+%; TLC (EtOAc/hexane = 1/9): R_f = 0.45; ^{1}H NMR (500 MHz, $CDCl_3$, 27 ℃, TMS): δ = 7.65 (dd, 1H, *J* = 6.5, 2.0 Hz), 7.54 (s, 1H), 6.88 (d, 1H, *J* = 8.5 Hz), 4.09-4.04 (m, 4H), 3.88 (s, 3H), 1.87-1.80 (m, 2H), 1.63 (m, 4H), 1.47 (m, 2H), 1.33-1.31 (m, 6H), 1.17-1.14 (m, 6H), 0.94 (d, 6H, *J* = 6.5 Hz), 0.87 (d, 12H, *J* = 6.6 Hz); ^{13}C NMR (125 MHz, 27 ℃, $CDCl_3$): δ = 167.2, 153.3, 148.7, 123.7, 122.5, 114.1, 111.9, 67.7, 67.5, 53.6, 39.6, 37.5, 36.3, 30.1, 28.3, 24.9, 22.9, 22.8, 19.9 ppm.

***Racemic by Synthesis*-(3,4)dm8*G1-CO_2CH_3 (3).** This compound was synthesized by the same procedure described for the synthesis of compound **1**. From methyl 3,4-dihydroxybenzoate (1.00 g, 5.95 mmol), K_2CO_3 (3.29 g, 23.8 mmol) and *rac*-1-bromo-3,7-dimethyloctane (2.63 g, 11.9 mmol) in DMF (25 mL), compound **3** (1.09 g, 41%) was obtained as colorless viscous liquid. HPLC: 99+%; TLC (EtOAc/hexane = 1/9): R_f = 0.45; ^{1}H NMR (500 MHz, $CDCl_3$, 27 ℃, TMS): δ = 7.65 (dd, 1H, *J* = 6.5, 2.0 Hz), 7.54 (s, 1H), 6.88 (d, 1H, *J* = 8.5 Hz), 4.09-4.04 (m, 4H), 3.88 (s, 3H), 1.87-1.80 (m, 2H), 1.63 (m, 4H), 1.47 (m, 2H), 1.33-1.31 (m, 6H), 1.17-1.14 (m, 6H), 0.94 (d, 6H, *J* = 6.5 Hz), 0.87 (d, 12H, *J* = 6.6 Hz); ^{13}C NMR (125 MHz, 27 ℃, $CDCl_3$): δ = 167.2, 153.3, 148.7, 123.7, 122.5, 114.1, 111.9, 67.7, 67.5, 53.6, 39.6, 37.5, 36.3, 30.1, 28.3, 24.9, 22.9, 22.8, 19.9 ppm.

(3,4)8G1-CO_2CH_3 (4). This compound was synthesized by the same procedure described for the synthesis of compound **1**. From methyl 3,4-dihydroxybenzoate (1.72 g, 0.01 mol), K_2CO_3 (5.53 g, 0.04 mol) and 1-bromooctane (4.0 mL, 0.02 mol) in DMF (40 mL), compound **4** (3.32 g, 83%) was obtained as

colorless viscous liquid. HPLC: 99+%; TLC (EtOAc/hexane = 1/9): R_f = 0.45; ^{1}H NMR (500 MHz, $CDCl_3$, 27 ℃, TMS): δ = 7.63 (dd, 1H, *J* = 8.4, 2.0 Hz), 7.54 (d, 1H, *J* = 1.9 Hz), 6.86 (d, 1H, *J* = 8.4 Hz), 4.04 (t, 2H, *J* = 6.6 Hz), 4.03 (t, 2H, *J* = 6.6 Hz), 3.87 (s, 3H), 1.83 (m, 4H), 1.47 (m, 4H), 1.32-1.28 (m, 16H), 0.88 (t, 6H, *J* = 6.2 Hz); ^{13}C NMR (125 MHz, 27 ℃, $CDCl_3$): δ = 167.3, 153.6, 148.9, 123.9, 122.8, 114.6, 112.3, 69.6, 69.4, 52.2, 32.2, 32.1, 29.7, 29.6, 29.5, 29.4, 26.3, 23.0, 14.4 ppm.

(3,4)12G1-CO_2CH_3 (5). This compound was synthesized by the same procedure described for the synthesis of compound **1**. From methyl 3,4-dihydroxybenzoate (1.68 g, 0.01 mol), K_2CO_3 (5.53 g, 0.04 mol) and 1-bromododecane (5.3 mL, 0.02 mol) in DMF (40 mL), compound **5** (4.99 g, 99%) was obtained as colorless viscous liquid. HPLC: 99+%; TLC (EtOAc/hexane = 1/9): R_f = 0.45; ^{1}H NMR (500 MHz, $CDCl_3$, 27 ℃, TMS): δ = 7.62 (dd, 1H, *J* = 8.4, 2.0 Hz), 7.53 (d, 1H, *J* = 2.0 Hz), 6.85 (d, 1H, *J* = 8.5 Hz), 4.03 (t, 4H, *J* = 6.6 Hz), 3.86 (s, 3H), 1.82 (m, 4H), 1.46 (m, 4H), 1.31-1.26 (m, 32H), 0.88 (t, 6H, *J* = 6.8 Hz); ^{13}C NMR (125 MHz, 27 ℃, $CDCl_3$): δ = 167.2, 153.5, 148.8, 123.8, 122.7, 114.6, 112.2, 69.6, 69.3, 52.1, 32.2, 30.0, 29.9, 29.7, 29.5, 29.4, 26.3, 23.0, 14.4 ppm.

***(S)*-(3,4)dm8*G1-CH_2Cl (6).** To a slurry of $LiAlH_4$ (0.40 g, 11 mmol) in dry THF (20 mL) at 0 ℃ was slowly added the ester **1** (3.14 g, 7.0 mmol) in dry THF (15 mL) over 30 min under nitrogen. The mixture was stirred at room temperature for 2 h, after which TLC (CH_2Cl_2) showed completion. The reaction mixture was cooled to 0 ℃ and quenched by successive addition of H_2O (1 mL), 15% aq. NaOH (1 mL) and H_2O (3 mL) with continuous stirring until H_2 evolution ceased. The reaction mixture was then filtered through celite and the lithium salts were rinsed generously with THF. The filtrate was dried over Na_2SO_4 and concentrated to give ***(S)*-(3,4)dm8*G1-CH_2OH** (2.75 g, 94%) as colorless viscous oil.

Thionyl chloride (0.35 mL, 4.4 mmol in 5 mL of dry CH_2Cl_2) was added dropwise under nitrogen to a 0 ℃ solution of ***(S)*-(3,4)dm8*G1-CH_2OH** (1.48 g, 3.5 mmol) in dry CH_2Cl_2 (20 mL) with a catalytic amount of DMF (0.2 mL). Upon addition, reaction was allowed to stir for 20 min, while monitoring through TLC (CH_2Cl_2) for completion. The reaction mixture was concentrated under reduced pressure and the residue was taken up with ether. The product was washed with H_2O and brine, then dried over anhydrous $MgSO_4$ and concentrated to give ***(S)*-(3,4)dm8*G1-CH_2Cl** (**6**) as a colorless oil (1.47 g, 96%). HPLC: 99%; TLC (EtOAc/hexane = 3/7): R_f = 0.84; ^{1}H NMR (500 MHz, $CDCl_3$, 27 ℃, TMS): δ = 6.92-6.89 (overlapped peaks, 2H), 6.84 (d, 1H, *J* = 8.1 Hz), 4.55 (s, 2H), 4.06-3.99 (overlapped t, 4H, *J* = 6.0 Hz), 1.85 (m, 2H), 1.69-1.62 (m, 4H), 1.53 (m, 2H), 1.33-1.30 (m, 6H), 1.17-1.14 (m, 6H), 0.96 (d, 6H, *J* = 6.4 Hz), 0.88 (d, 12H, *J* = 6.6 Hz); ^{13}C NMR (125 MHz, 27 ℃, $CDCl_3$): δ = 149.6, 149.5, 130.2, 121.5, 114.3, 113.6, 67.8, 47.0, 39.5, 37.6, 36.5, 30.2, 28.2, 24.9, 22.9, 22.8, 19.9 ppm.

***(R)*-(3,4)dm8*G1-CH_2Cl (7).** This compound was synthesized by the same procedure described for the synthesis of compound **6**. From $LiAlH_4$ (0.31 g, 8.3 mmol) in dry THF (15 mL) and **2** (2.47 g, 5.5 mmol) in dry THF (15 mL), ***(R)*-(3,4)dm8*G1-CH_2OH** was obtained (2.2 g, 95%) as colorless viscous oil.

From $SOCl_2$ (0.27 mL, 3.8 mmol in 5 mL of dry CH_2Cl_2) and ***(R)*-(3,4)dm8*G1-CH_2OH** (1.26 g, 3.0 mmol) in dry CH_2Cl_2 (20 mL) with a catalytic amount of dry DMF, compound **7** was obtained (1.31 g, 99%) as colorless oil. HPLC: 99%; TLC (EtOAc/hexane = 3/7): R_f = 0.84; ^{1}H NMR (500 MHz, $CDCl_3$, 27 ℃, TMS): δ = 6.92-6.89 (overlapped peaks, 2H), 6.84 (d, 1H, J = 8.1 Hz), 4.55 (s, 2H), 4.06-3.99 (overlapped t, 4H, J = 6.0 Hz), 1.85 (m, 2H), 1.69-1.62 (m, 4H), 1.53 (m, 2H), 1.33-1.30 (m, 6H), 1.17-1.14 (m, 6H), 0.96 (d, 6H, J = 6.4 Hz), 0.88 (d, 12H, J = 6.6 Hz); ^{13}C NMR (125 MHz, 27 ℃, $CDCl_3$): δ = 149.6, 149.5, 130.2, 121.5, 114.3, 113.6, 67.8, 47.0, 39.5, 37.6, 36.5, 30.2, 28.2, 24.9, 22.9, 22.8, 19.9 ppm.

***Racemic by Synthesis*-(3,4)dm8*G1-CH_2Cl (8).** This compound was synthesized by the same procedure described for the synthesis of compound **6**. From $LiAlH_4$ (0.14 g, 3.6 mmol) in dry THF (5 mL) and **3** (1.08 g, 2.4 mmol) in dry THF (5 mL), ***Racemic by Synthesis* -(3,4)dm8*G1-CH_2OH** was obtained (0.88 g, 87%) as colorless viscous oil.

From $SOCl_2$ (0.19 mL, 2.7 mmol in 3 mL of dry CH_2Cl_2) and ***Racemic by Synthesis* -(3,4)dm8*G1-CH_2OH** (0.88 g, 2.1 mmol) in dry CH_2Cl_2 (15 mL) with a catalytic amount of dry DMF, compound **8** was obtained (0.85 g, 93%) as colorless oil. HPLC: 99%; TLC (EtOAc/hexane = 3/7): R_f = 0.84; ^{1}H NMR (500 MHz, $CDCl_3$, 27 ℃, TMS): δ = 6.92-6.89 (overlapped peaks, 2H), 6.84 (d, 1H, J = 8.1 Hz), 4.55 (s, 2H), 4.06-3.99 (overlapped t, 4H, J = 6.0 Hz), 1.85 (m, 2H), 1.69-1.62 (m, 4H), 1.53 (m, 2H), 1.33-1.30 (m, 6H), 1.17-1.14 (m, 6H), 0.96 (d, 6H, J = 6.4 Hz), 0.88 (d, 12H, J = 6.6 Hz); ^{13}C NMR (125 MHz, 27 ℃, $CDCl_3$): δ = 149.6, 149.5, 130.2, 121.5, 114.3, 113.6, 67.8, 47.0, 39.5, 37.6, 36.5, 30.2, 28.2, 24.9, 22.9, 22.8, 19.9 ppm.

(3,4)8G1-CH_2Cl (9). This compound was synthesized by the same procedure described for the synthesis of compound **6**. From $LiAlH_4$ (0.39 g, 10 mmol) in dry THF (30 mL) and **4** (3.0 g, 7.6 mmol) in dry THF (30 mL), **(3,4)8G1-CH_2OH** was obtained (2.8 g, 95%) as colorless viscous oil.

From $SOCl_2$ (0.96 mL, 13 mmol in 10 mL of dry CH_2Cl_2) and **(3,4)8G1-CH_2OH** (2.8 g, 7.2 mmol) in dry CH_2Cl_2 (30 mL) with a catalytic amount of dry DMF, compound **9** was obtained (2.3 g, 78%) as colorless solid. HPLC: 99%; TLC (EtOAc/hexane = 3/7): R_f = 0.8; ^{1}H NMR (500 MHz, $CDCl_3$, 27 ℃, TMS): δ = 6.92 (d, 1H, J = 2.0 Hz), 6.89 (dd, 1H, J = 8.1 Hz, J = 2.1 Hz), 6.82 (d, 1H, J = 8.1 Hz), 4.55 (s, 2H), 4.00 (t, 2H, J = 6.6 Hz), 3.99 (t, 2H, J = 6.6 Hz), 1.81 (m, 4H), 1.46 (m, 4H), 1.29 (m, 16H), 0.90 (t, 6H, J = 5.7 Hz); ^{13}C NMR (125 MHz, 27 ℃, $CDCl_3$): δ = 149.8, 149.6, 130.4, 121.6, 114.6, 113.9, 69.7, 69.6, 47.1, 32.2, 29.7, 29.6, 26.4, 26.3, 23.0, 14.4 ppm.

(3,4)12G1-CH_2Cl (10). This compound was synthesized by the same procedure described for the synthesis of compound **6**. From $LiAlH_4$ (0.27 g, 10 mmol) in dry THF (25 mL) and **5** (2.9 g, 5.7 mmol) in dry THF (15 mL), **(3,4)12G1-CH_2OH** was obtained (2.7 g, 94%) as colorless viscous oil.

From $SOCl_2$ (0.50 mL, 6.9 mmol in 10 mL of dry CH_2Cl_2) and **(3,4)12G1-CH_2OH** (2.7 g, 5.4 mmol) in dry CH_2Cl_2 (30 mL) with a catalytic amount of dry DMF, compound **9** was obtained (2.7 g, 95%) as colorless solid. HPLC: 99%; TLC (EtOAc/hexane = 3/7): R_f = 0.8; ^{1}H NMR (500 MHz, $CDCl_3$, 27 ℃, TMS): δ = 6.92 (d, 1H, J = 2.0 Hz), 6.90 (dd, 1H, J = 8.2 Hz, J = 2.0 Hz), 6.83 (d, 1H, J = 8.1 Hz), 4.55 (s, 2H), 4.01 (t, 2H, J = 6.7 Hz), 3.99 (t, 2H, J = 6.7 Hz), 1.82 (m, 4H), 1.48 (m, 4H), 1.34-1.28 (m, 32H), 0.90 (t, 6H, J = 6.8 Hz); ^{13}C NMR (125 MHz, 27 ℃, $CDCl_3$): δ = 149.8, 149.6, 130.4, 121.6, 114.6, 113.9, 69.6, 47.0, 32.3, 30.0, 29.8, 29.7, 29.6, 26.4, 23.0, 14.4 ppm.

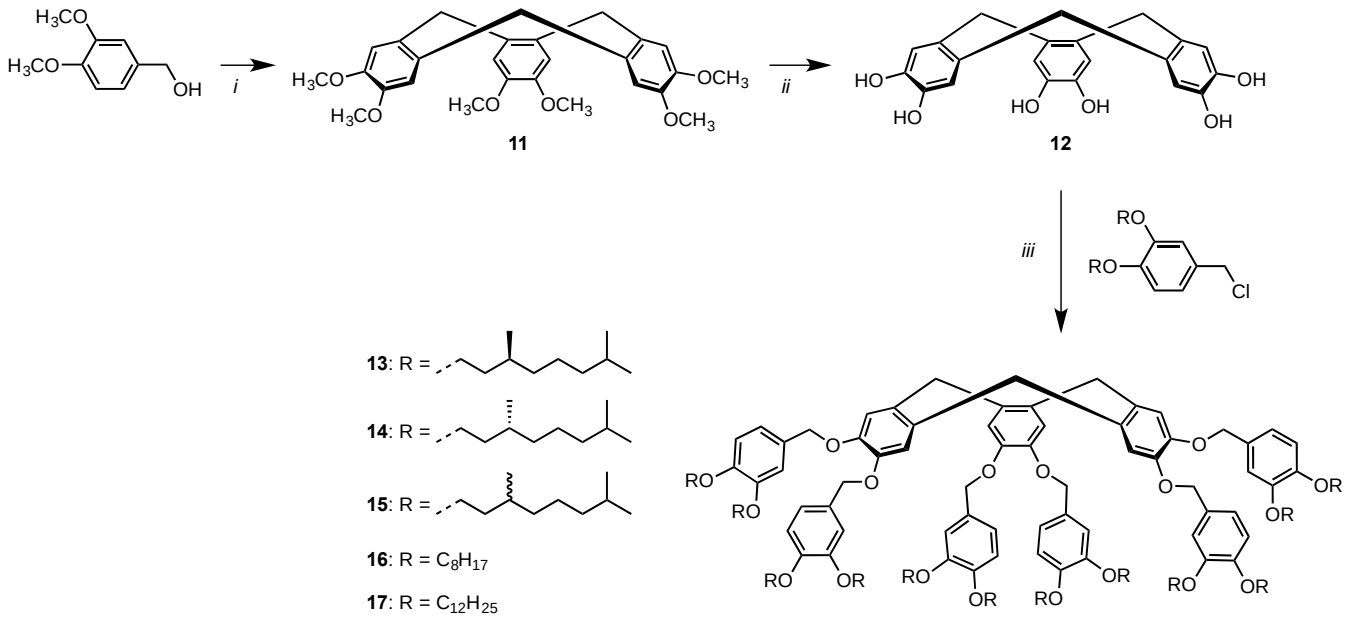

Supporting Scheme SS2. Synthesis of dendronized cyclotriveratrylene (CTV) derivatives **13-17**. Reagents and conditions: *(i)* H_3PO_4, 80 ℃, 5 h; *(ii)* BBr_3, CH_2Cl_2, reflux, 2 h; *(iii)* K_2CO_3, DMF, 80 ℃, 16 h.

Cyclotriveratrylene (CTV) (11). Veratryl alcohol (10.09 g, 0.06 mol) was placed in a round bottom flask and heated in an oil bath to 80 ℃. A few drops of H_3PO_4 were added and the reaction mixture was stirred for 5 h. The reaction mixture was cooled to room temperature and the pale yellow solid was added to methanol (100 mL) while stirring. The crude solid was collected by filtration and recrystallized from dichloromethane/methanol to yield 2.8 g (31%) of pure white crystal. M.p. 230-231 ℃; TLC (CH_2Cl_2/EtOH = 9/1): R_f = 0.65; ^{1}H NMR (500 MHz, $CDCl_3$, 27℃, TMS): δ = 3.56 (H_{eq}) and 4.78 (H_{ax})

(d, 6H, Ar*CH*$_2$Ar), 3.84 (s, 18H, *OCH*$_3$), 6.83 (s, 6H, Ar-*H*); ^{13}C NMR (125 MHz, $CDCl_3$, 27 ℃, TMS): δ = 36.7, 56.2, 113.4, 132.0, 147.9.

CTV(OH)$_6$ (12). Into a stirred solution of CTV (2.52 g, 5 mmol) in dry CH_2Cl_2 (40 mL) at 0 ℃, BBr_3 (3.3 mL, 35 mmol in 20 mL of dry CH_2Cl_2) was added dropwise under nitrogen. The slightly purple reaction mixture was stirred at 0 ℃ for 15 min, at RT for 10 min, and then refluxed for 2 h. The reaction mixture was quenched by slow addition 20-25 mL H_2O at 0 ℃. The resulting slurry was filtered under nitrogen and washed with H_2O. The crude wet solid was recrystallized from aqueous EtOH to yield 1.52 g (83%) of slightly brownish prism-like crystals. M.p. > 325 ℃ (decompose)[6]: 375 ℃, decomp.); ^{1}H NMR (500 MHz, $CDCl_3$-DMSO-d_6, 27℃, TMS): δ = 2.39 (H_{eq}) and 3.63 (H_{ax}) (d, 6H, Ar*CH*$_2$Ar), 5.80 (s, 6H, *OH*), 7.52 (s, 6H, Ar-*H*); ^{13}C NMR (125 MHz, $CDCl_3$-DMSO-d_6, 27 ℃, TMS): δ = 34.2, 115.5, 129.8, 142.2.

General Procedure for the Synthesis of Dendronized CTV Derivatives. To a thoroughly degassed suspension of anhydrous K_2CO_3 (12 equiv.) in DMF was added CTV(OH)$_6$ (1 equiv.) and the resulting mixture was heated to 80 ℃ with continuous degassing. At 60 ℃ was added the dendritic chloride (6 equiv.) and the reaction allowed to stir 80 ℃ under N_2 for 8-16 h (TLC controlled). The reaction mixture was cooled to room temperature and poured into cold water. The precipitate was collected by vacuum filtration (or extracted with CH_2Cl_2, if necessary) and passed through basic alumina using DCM as eluent. The crude product was then purified by a combination of column chromatography (silica gel, CH_2Cl_2 or EtOAc/hexane) and precipitation from MeOH or recrystallization from acetone.

***(S)*-(3,4)dm8*G1-CTV (13).** From CTV(OH)$_6$ **12** (165 mg, 0.45 mmol), K_2CO_3 (750 mg, 5.4 mmol), and ***(S)*-(3,4)dm8*G1-CH$_2$Cl 6** (1.19 g, 2.7 mmol) in DMF (20 mL) for 16 h at 80 ℃, 0.68 g (54%) of **13** was obtained as a white solid after precipitation in MeOH. HPLC: 99+%; TLC (EtOAc/hexane = 1/9): R_f = 0.33; ^{1}H NMR (500 MHz, $CDCl_3$, 27 ℃, TMS): δ = 0.84 (d, 36H, *(CH$_3$)$_2$*, *J* = 6.5 Hz), 0.86 (d, 36H, *(CH$_3$)$_2$*, *J* = 6.5 Hz), 0.88 (d, 18H, *CH$_3$*, *J* = 6.5 Hz), 0.92 (d, 18H, *CH$_3$*, *J* = 6.5 Hz), 1.14 (m, 36H), 1.29-1.33 (m, 36H), 1.53 (m, 24H), 1.65 (m, 12H, $(CH_3)_2$*CH*), 1.82 (m, 12H, CH_3*CH*), 3.45 (d, 3H, Ar*CH*$_2$Ar, H_{eq}, *J* = 13.7 Hz), 3.89-3.99 (overlapped t, 24H, *CH*$_2$OAr), 4.67 (d, 3H, Ar*CH*$_2$Ar, H_{ax}, *J* = 13.6 Hz), 4.96 (dd, 12H, Ar*CH*$_2$O, *J* = 19.1, 11.4 Hz), 6.81 (d, 6H, 2', position, *J* = 8.2 Hz), 6.91 (overlapped d, 12H, 5',6' position), 6.97 (s, 6H, Ar*H*) ppm; ^{13}C NMR (125 MHz, $CDCl_3$, 27 ℃, TMS): δ = 19.8, 19.9, 22.8, 22.9, 25.0, 28.2, 30.1, 30.2, 36.6, 37.7, 39.5, 67.7, 67.9, 72.4, 113.5, 113.8, 118.0, 120.4, 130.3, 133.2, 148.4, 149.1, 149.5 ppm; MALDI-TOF *m/z*: 2804.85 ($[M+Na]^+$, calculated for $C_{207}H_{342}O_{18}Na$ 2805.27).

***(R)*-(3,4)dm8*G1-CTV (14).** From CTV(OH)$_6$ **12** (49 mg, 0.14 mmol), K_2CO_3 (225 mg, 1.6 mmol), and ***(R)*-(3,4)dm8*G1-CH$_2$Cl 7** (0.37 g, 0.85 mmol) in DMF (10 mL) for 16 h at 80 ℃, 0.12 g (31%) of **14**

was obtained as a white solid after precipitation in MeOH. HPLC: 99+%; TLC (EtOAc/hexane = 1/9): R_f = 0.33; ^{1}H NMR (500 MHz, $CDCl_3$, 27 ℃, TMS): δ = 0.85 (d, 36H, *(CH$_3$)$_2$*, *J* = 6.5 Hz), 0.86 (d, 36H, *(CH$_3$)$_2$*, *J* = 6.5 Hz), 0.88 (d, 18H, *CH$_3$*, *J* = 6.5 Hz), 0.92 (d, 18H, *CH$_3$*, *J* = 6.5 Hz), 1.13 (m, 36H), 1.27-1.32 (m, 36H), 1.53-1.60 (m, 24H), 1.65 (m, 12H, $(CH_3)_2CH$), 1.82 (m, 12H, CH_3CH), 3.45 (d, 3H, Ar*CH$_2$*Ar, H_{eq}, *J* = 13.7 Hz), 3.89-3.99 (overlapped t, 24H, *CH$_2$*OAr), 4.67 (d, 3H, Ar*CH$_2$*Ar, H_{ax}, *J* = 13.6 Hz), 4.96 (dd, 12H, Ar*CH$_2$*O, *J* = 19.1, 11.4 Hz), 6.81 (d, 6H, 2', position, *J* = 8.2 Hz), 6.92 (overlapped d, 12H, 5',6' position), 6.97 (s, 6H, Ar*H*) ppm; ^{13}C NMR (125 MHz, $CDCl_3$, 27 ℃, TMS): δ = 19.8, 19.9, 22.8, 22.9, 25.0, 28.2, 30.1, 30.2, 36.6, 37.7, 39.5, 67.7, 67.9, 72.4, 113.6, 113.8, 118.0, 120.4, 130.3, 133.2, 148.4, 149.1, 149.5 ppm; MALDI-TOF *m/z*: 2804.13 ($[M+Na]^+$, calculated for $C_{207}H_{342}O_{18}Na$ 2805.27).

***Racemic by Synthesis* -(3,4)dm8*G1-CTV (15).** From $CTV(OH)_6$ **12** (0.12 g, 0.31 mmol), K_2CO_3 (0.53 g, 3.8 mmol), and ***Racemic by Synthesis* -(3,4)dm8*G1-CH$_2$Cl 8** (0.83 g, 1.9 mmol) in DMF (15 mL) for 16 h at 80 ℃, 0.29 g (23%) of **15** was obtained as a white solid after precipitation in MeOH. HPLC: 99+%; TLC (EtOAc/hexane = 1/9): R_f = 0.33; ^{1}H NMR (500 MHz, $CDCl_3$, 27 ℃, TMS): δ = 0.85 (d, 36H, *(CH$_3$)$_2$*, *J* = 6.5 Hz), 0.86 (d, 36H, *(CH$_3$)$_2$*, *J* = 6.5 Hz), 0.88 (d, 18H, *CH$_3$*, *J* = 6.5 Hz), 0.92 (d, 18H, *CH$_3$*, *J* = 6.5 Hz), 1.13 (m, 36H), 1.27-1.32 (m, 36H), 1.50-1.59 (m, 24H), 1.65 (m, 12H, $(CH_3)_2CH$), 1.82 (m, 12H, CH_3CH), 3.45 (d, 3H, Ar*CH$_2$*Ar, H_{eq}, *J* = 13.7 Hz), 3.89-3.99 (overlapped t, 24H, *CH$_2$*OAr), 4.67 (d, 3H, Ar*CH$_2$*Ar, H_{ax}, *J* = 13.6 Hz), 4.96 (dd, 12H, Ar*CH$_2$*O, *J* = 19.1, 11.4 Hz), 6.81 (d, 6H, 2', position, *J* = 8.2 Hz), 6.92 (overlapped d, 12H, 5',6' position), 6.97 (s, 6H, Ar*H*) ppm; ^{13}C NMR (125 MHz, $CDCl_3$, 27 ℃, TMS): δ = 19.8, 19.9, 22.8, 22.9, 24.9, 28.2, 30.1, 30.2, 36.6, 37.7, 39.5, 67.7, 67.9, 72.4, 113.6, 113.8, 118.0, 120.4, 130.3, 133.2, 148.4, 149.1, 149.5 ppm; MALDI-TOF *m/z*: 2805.26 ($[M+Na]^+$, calculated for $C_{207}H_{342}O_{18}Na$ 2805.27).

(3,4)8G1-CTV (16). From $CTV(OH)_6$ **12** (0.12 g, 0.31 mmol), K_2CO_3 (0.53 g, 3.8 mmol), and **(3,4)8G1-CH$_2$Cl 9** (0.83 g, 1.9 mmol) in DMF (15 mL) for 16 h at 80 ℃, 0.22 g (20%) of **16** was obtained as a white solid after precipitation in MeOH. HPLC: 99+%; TLC (EtOAc/hexane = 1/9): R_f = 0.33; ^{1}H NMR (500 MHz, $CDCl_3$, 27 ℃, TMS): δ = 0.87 (overlapped t, 36H, *CH$_3$*), 1.25-1.31 (m, 84H, *CH$_2$*), 1.43 (m, 24H), 1.76 (m, 24H), 3.45 (d, 3H, Ar*CH$_2$*Ar, H_{eq}, *J* = 13.7 Hz), 3.86-3.94 (overlapped t, 24H, *CH$_2$*OAr), 4.67 (d, 3H, Ar*CH$_2$*Ar, H_{ax}, *J* = 13.6 Hz), 4.96 (dd, 12H, Ar*CH$_2$*O, *J* = 19.1, 11.4 Hz), 6.80 (d, 6H, 2', position, *J* = 8.2 Hz), 6.91 (overlapped d, 12H, 5',6' position), 6.96 (s, 6H, Ar*H*) ppm; ^{13}C NMR (125 MHz, $CDCl_3$, 27 ℃, TMS): δ = 14.3, 22.9, 26.2, 26.3, 29.5, 29.6, 29.7, 32.1, 36.7, 37.7, 39.5, 69.3, 69.5, 72.4, 113.6, 113.8, 117.9, 120.3, 130.3, 133.1, 148.3, 149.1, 149.5 ppm; MALDI-TOF *m/z*: 2469.90 ($[M+Na]^+$, calculated for $C_{159}H_{246}O_{18}Na$ 2468.69).

(3,4)12G1-CTV (17). From $CTV(OH)_6$ **12** (147 mg, 0.4 mmol), K_2CO_3 (662 mg, 4.8 mmol), and **(3,4)12G1-CH_2Cl 10** (1.19 g, 2.4 mmole) in DMF (20 mL) for 16 h at 80 ℃, 0.70 g (56%) of pale white solid was obtained after precipitation in MeOH. HPLC: 99+%; TLC (EtOAc/hexane = 1/9): R_f = 0.56; ^{1}H NMR (500 MHz, $CDCl_3$, 27 ℃, TMS): δ = 0.89 (t, 36H, *CH_3*, *J* = 6.8 Hz), 1.26 (overlapped m, 192H, $CH_3(CH_2)_8$), 1.41-1.44 (m, 24H, *CH_2*$(CH_2)_2O$), 1.72-1.78 (m, 24H, *CH_2*CH_2O), 3.47 (d, 3H, Ar*CH_2*Ar, H_{eq}, *J* = 13.7 Hz), 3.86-3.94 (overlapped t, 24H, *CH_2*OAr), 4.68 (d, 3H, Ar*CH_2*Ar, H_{ax}, *J* = 13.5 Hz), 4.92-5.00 (dd, 12H, Ar*CH_2*O, *J* = 17.7, 11.4 Hz), 6.80 (d, 6H, 2', position, *J* = 8.2 Hz), 6.91 (overlapped, 12H, 5',6' position), 6.96 (s, 6H, Ar*H*); ^{13}C NMR (125 MHz, $CDCl_3$, 27 ℃, TMS): δ = 14.3, 22.9, 26.3, 29.6-30.0, 32.2, 36.7, 69.4, 69.6, 72.4, 113.6, 113.9, 117.9, 120.4, 130.3, 133.2, 148.4, 149.1, 149.5; MALDI-TOF *m/z*: 3142.48 ($[M+Na]^+$, calculated for $C_{207}H_{342}O_{18}Na$ 3141.91), 3159.19 ($[M+K]^+$, calculated 3158.02).

4. Comparison of Conglomerates of Low Molar Mass Compounds and Self-Assembling Building Blocks

The crystallization of racemic mixtures of low molar mass *R* and *S* compounds into racemic compound, conglomerate, and solid solution in shown in Supporting Scheme SS3.[7]

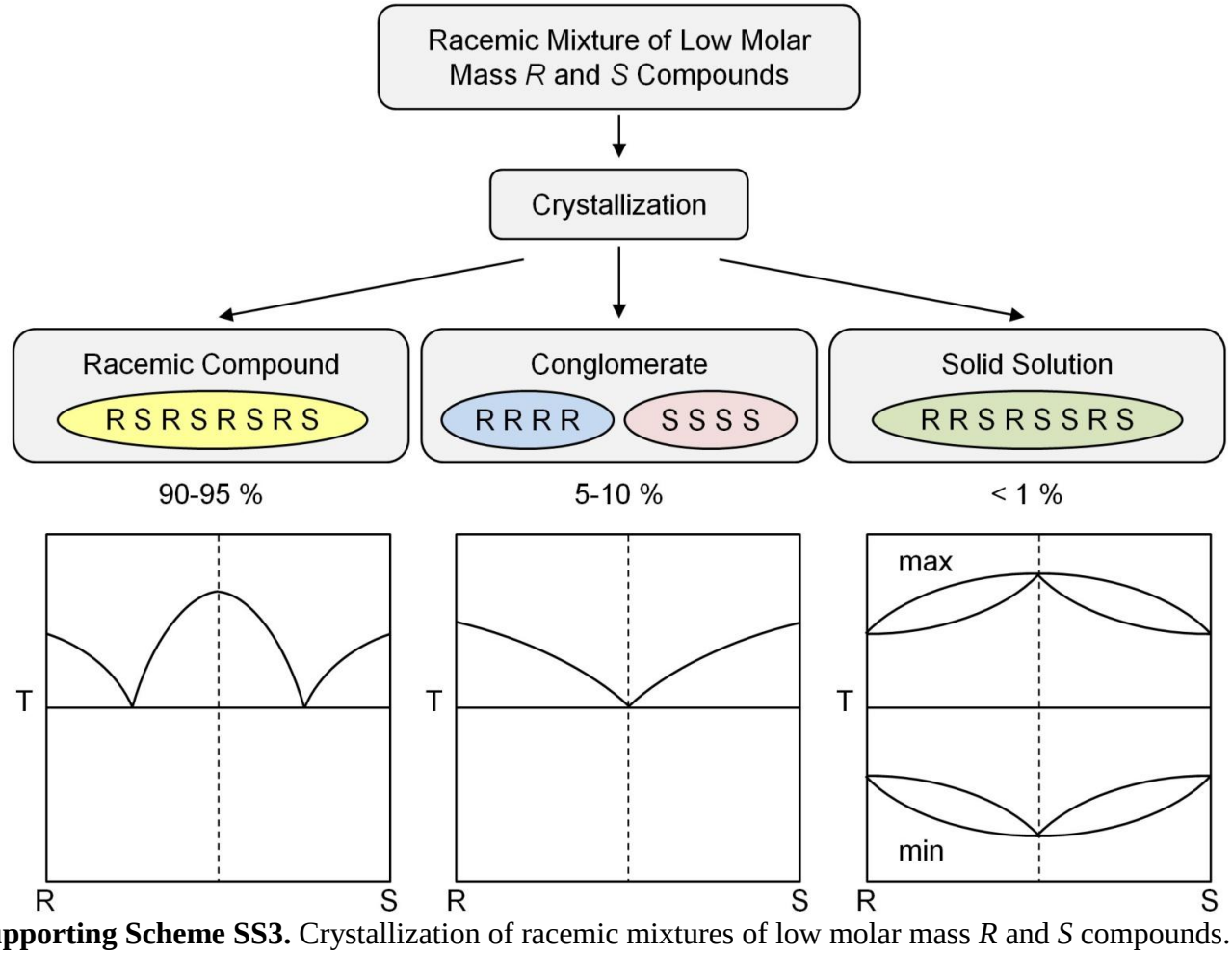

Supporting Scheme SS3. Crystallization of racemic mixtures of low molar mass *R* and *S* compounds.

5. Thermal Analysis by DSC

With mixtures of chiral and achiral molecules, the isotropic temperature increased significantly due to the decreased amount of branched alkyl chains (Supporting Figure SF1). However, no crystal structure was observed in the whole temperature range, indicating the mixing of molecules with long linear chains in columns would make them difficult to register with each other and destroy completely the inter-column correlations.

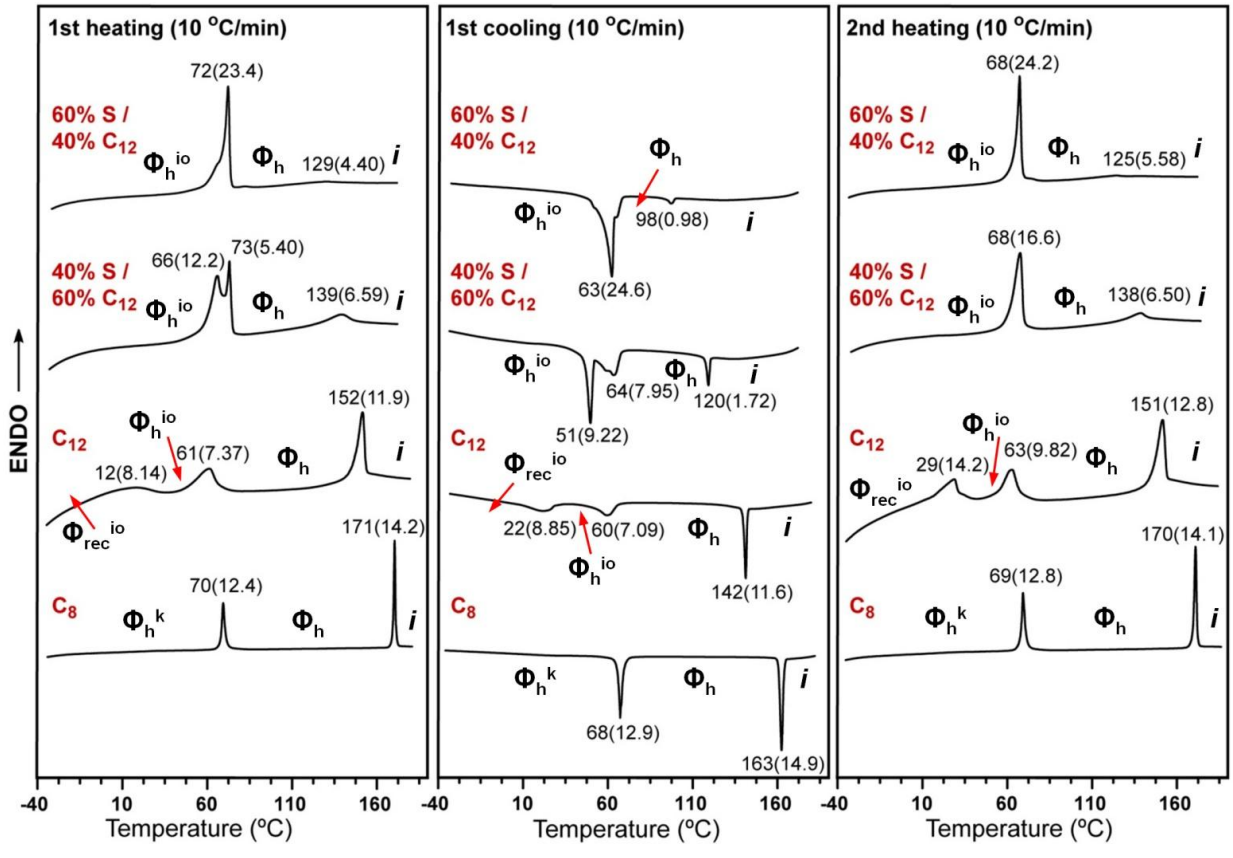

Supporting Figure SF1. DSC traces of chiral and linear achiral CTVs with different blending compositions recorded with heating and cooling rates of 10 °C/min. Phases, transition temperatures, and associated enthalpy changes (in brackets in kcal/mol) are indicated.

Similarly, no crystalline phase was observed for the pure achiral 12-carbon CTV sample since the core-core correlation is more difficult to be established when the CTV cores are embedded within the envelope of long amorphous alkyl chains. However, the linear side chains make the 2D hexagonal phase much more stable (higher melting temperature, 152 °C) than that generated with branching chiral chains, indicating more stable intra-column core stacking is achieved with linear side chains. The achiral CTV with 8-carbon side chains, on the other hand, can form a crystal structure at room temperature but with poorer order. This indicates that the crystal order is improved with shorter chain length but high inter-column correlation cannot be obtained without chiral side chains and good phase separation of columns with opposite handedness. The shorter alkyl side chains also make the isotropic temperature increase to 170 °C.

Additional Discussion for DSC Traces Listed in Figure 2 of Main Text

This discussion refers to Figure 2 in the main text. As in previously reported assemblies (dendritic dipeptide)[8] a decrease of the enantiomeric excess of the supramolecular column decreases the melting temperature of the Φ_h^k phase. When mixing both enantiomers with a 3:1 ratio, although the majority of columns possess the same handedness, but less enantiomerically pure columns lead to less ordered crystals with melting temperature a few degrees lower than that found in pure enantiomers. A small portion of columns consist of high mixing level of two enantiomers or of opposite rotation sense and therefore generate crystal with even lower order. With a mixture of 1:1 *R/S* ratio, the incompatible packing between columns becomes more remarkable since more columns contain high level of randomly arranged *R* and *S* enantiomers. The columns with inhomogeneous compositions and different handedness form crystals of different stability that manifested in the broad multi-peak DSC feature. Imperfect mixing of two enantiomers takes place in an early stage of self-assembly since the association constant of the same enantiomer is higher than that of different enantiomers. Therefore, the columns formed first are enantiomerically rich and pack into better ordered crystals that give the sharpest peak with the highest transition temperature. In a later stage, columns are formed with more randomly arranged enantiomers and pack into crystals with higher defect density and lower melting point. Finally, the most disordered columns that are not able to pack well with each other form the least stable crystals with the lowest melting temperature. The molecules have a tendency to phase separate into enantiomerically pure columns in order to achieve better crystal order (lower energy).

Supporting Table ST1. Thermal Transitions and Associated Enthalpy Changes of Chiral and Linear CTVs Determined by DSC and XRD.

m	Thermal transition (℃) and corresponding enthalpy changes (kcal/mol)	
	Heating[a]	Cooling
(3,4)dm8*G1-CTV 100% R	Φ_h^k 73 (29.2) Φ_h 79 (1.87) i Φ_h^k 74 (31.9) Φ_h 79 (1.73) i	i 70 (-2.45) Φ_h 64 (-28.4) Φ_h^k
(3,4)dm8*G1-CTV 100% S	Φ_h^k 72 (26.9) Φ_h 79 (1.88) i Φ_h^k 73 (32.3) Φ_h 78 (1.73) i	i 68 (-2.79) Φ_h 64 (-28.4) Φ_h^k
(3,4)dm8*G1-CTV 75% R + 25% S	Φ_h^k 69 (17.8) Φ_h 80 (2.25) i Φ_h^k 69 (19.7) Φ_h 79 (1.96) i	i 68 (-3.09) Φ_h 59 (-22.9) Φ_h^k
(3,4)dm8*G1-CTV 75% S + 25% R	Φ_h^k 69 (17.7) Φ_h 80 (2.19) i Φ_h^k 67 (16.5) Φ_h 79 (2.08) i	i 69 (-3.35) Φ_h 57 (-19.6) Φ_h^k
(3,4)dm8*G1-CTV 50% R + 50% S	Φ_h^k 68 (15.2) Φ_h 80 (1.86) i Φ_h^k 66 (3.64) Φ_h 79 (1.92) i	i 70 (-2.94) Φ_h 41 (-12.8) Φ_h^k
(3,4)dm8*G1-CTV *racemic by synthesis*	Φ_h^{io} 44 (12.0) Φ_h 80 (3.22) i Φ_h^{io} 37 (11.2) Φ_h 80 (3.21) i	i 62 (-3.95) Φ_h 34 (-11.4) Φ_h^{io}
(3,4)dm8*G1-CTV 60% S (3,4)12G1-CTV 40% C_{12}	Φ_h^{io} 72 (23.4) Φ_h 129 (4.40) i Φ_h^{io} 68 (24.2) Φ_h 125 (5.58) i	i 98 (-0.98) Φ_h 63 (-24.6) Φ_h^{io}
(3,4)dm8*G1-CTV 40% S (3,4)12G1-CTV 60% C_{12}	Φ_h^{io} 66 (12.2) Φ_h 139 (6.59) i Φ_h^{io} 68 (16.6) Φ_h 138 (6.50) i	i 120 (-1.72) Φ_h 51 (-9.22) Φ_h^{io}
(3,4)12G1-CTV linear achiral chain	Φ_{rec}^{io} 12 (8.14) Φ_h^{io} 61 (7.37) Φ_h 152 (11.9) i Φ_{rec}^{io} 29 (14.2) Φ_h^{io} 63 (9.82) Φ_h 151 (12.8) i	i 142 (-11.6) Φ_h 60 (-7.09) Φ_h^{io} 22 (-8.85) Φ_{rec}^{io}
(3,4)8G1-CTV linear achiral chain	Φ_h^k 70 (12.4) Φ_h 171 (14.2) i Φ_h^k 69 (12.8) Φ_h 170 (14.1) i	i 163 (-14.9) Φ_h 68 (-12.9) Φ_h^k

[a] Data from the first heating and cooling scans are on the first line, and data from the second heating are on the second line. The scan rate was 10 ℃/min; Φ_h^k: three dimensional ordered columnar hexagonal phase, Φ_h^{io}: 2D columnar hexagonal phase with intracolumnar order, Φ_h: 2D columnar hexagonal phase without intracolumnar order, Φ_{rec}^{io}: 2D columnar rectangular phase with intracolumnar order, and i - isotropic. Note: quantitative uncertainties are ±1 ℃ for thermal transition temperatures and ~ 2% for the associated enthalpy changes reported in Kcal/mol.

Therefore by annealing at 60 ℃ for 2 h where the molecular motion is fast enough, spontaneous deracemization occurs and the resulting crystals have the same order as those formed by enantiomerically pure compounds. The "*racemic by synthesis*" sample, on the other hand, cannot achieve complete deracemization of enantiomers, and therefore, generates columns with random handedness and composition that pack into small domains with poor 3D order. The isotropic temperatures of all samples discussed above are quite similar regardless of chiral compositions. This suggests that at high temperature the supramolecular columns lose their helical conformation and intercolumnar order, and the structural stability becomes insensitive to molecular chirality.

The phase transition temperatures and associated phase structures determined by DSC and XRD for all tested samples are summarized in Supporting Table ST1.

6. Hexagonal Crystal Lattice Model and XRD Structural Analysis

XRD Analysis of Chiral and Achiral Mixtures Before and After Annealing

Mixing chiral and linear CTV compounds (Supporting Figure SF2a, b) generates only 2D ordered columnar structures with intra-columnar order. This suggests a similar core stacking feature compared with that of chiral side chains, but with the mixing of linear chains and chiral branched chains destroyed the helical conformation of the columns (absence of layer lines) and the long-range order between columns.

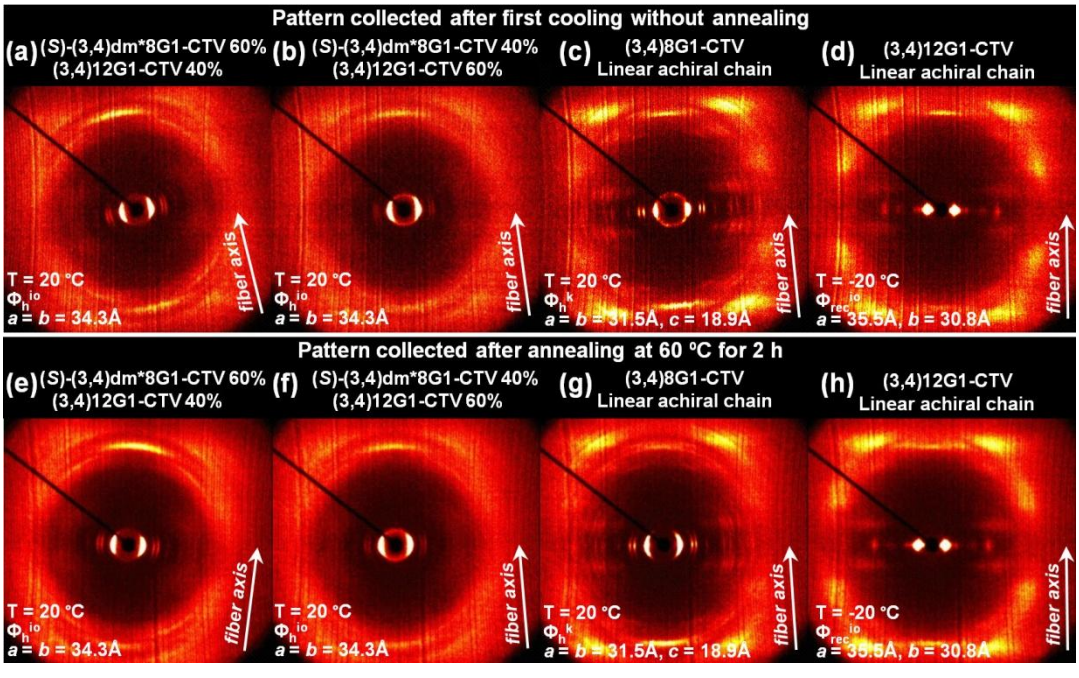

Supporting Figure SF2. Wide angle X-ray diffraction patterns collected from the oriented fibers of (a, b, e, f) mixture of chiral and achiral CTVs with indicated composition before and after annealing, and (c, d, g, h) CTVs with achiral linear side chains before and after annealing. Fiber axis, temperature, phase, and lattice dimensions are indicated.

CTVs with linear 12-carbon achiral side chains, however, cannot form crystalline structures due to the long and amorphous side chains, which greatly weaken the intercolumnar height-height ordering of the CTV cores. The 2D hexagonal LC structure is the stable phase in a wide temperature range above room temperature. At low temperature below RT, the hexagonal structure is transformed into a rectangular structure (Supporting Figure SF2c). The CTV compound with linear 8-carbon side chains, on the other hand, can form hexagonal crystals but with a smaller diameter (Supporting Figure SF2d). However, the crystal quality is much poorer than that formed by chiral counterparts. The XRD patterns obtained after annealing (bottom row in Supporting Figure SF2) are all similar to those obtained before annealing. This suggests that the annealing process does not improve the crystal order or thermal stability for samples containing achiral linear side chains since the complete deracemization of enantiomers cannot be achieved in these samples.

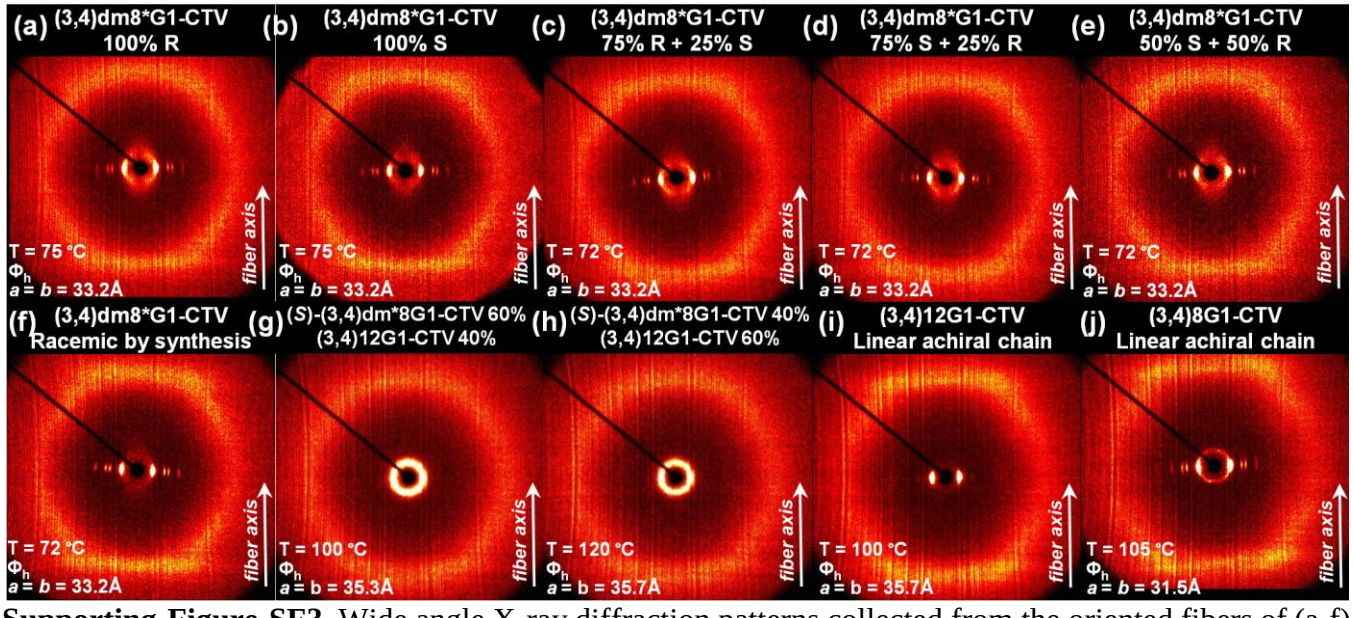

Supporting Figure SF3. Wide angle X-ray diffraction patterns collected from the oriented fibers of (a-f) chiral CTVs with indicated composition, (g, h) mixture of chiral and achiral CTVs with indicated composition, and linear achiral (3,4)nG1-CTV with (i) n = 8 and (j) n = 12 during second heating with a rate of 10 ℃/min at high temperature 2D hexagonal liquid crystalline phases. Fiber axis, temperature, phase, and lattice dimensions are indicated.

Supporting Figure SF3 shows the fiber XRD patterns of ten samples in their high temperature 2D Φ_h phase. At temperature above the crystalline-LC transition, all reflections and layer lines on quadrants have disappeared, indicating the loss of helical order in supramolecular columns, and also loss of 3D order between neighboring columns. On the equator, all samples with chiral chains (Supporting Figure SF3a to f) display sharp reflections, suggesting that good hexagonal 2D packing of columns is still preserved but that the columns are able to freely slide relative to each other. The column diameter is measured as 33.2 Å , which is slightly smaller than that found in the crystalline phase. The ring reflection found in samples with

mixtures of chiral and achiral compounds indicates that the columns have lost their orientational order in the Φ_h phase (Supporting Figure SF3g and h), since the temperature is higher than the isotropic temperature of their chiral component. However, upon decreasing the temperature back to RT, the columns are re-oriented along the fiber axis (Supporting Figure SF2a and b). This indicates there is a memory effect of orientation kept by the achiral molecules at high temperature, and that the achiral molecules can guide the orientation during supramolecular column assembly. CTVs with linear 8-carbon alkyl chains can form better ordered 2D columnar arrays compared to those with linear 12-carbon counterparts (Supporting Figure SF3i and j). This suggests that better column packing can be achieved with a thinner amorphous alkyl chain envelope surrounding the column core. All samples show fluctuations in the CTV core stacking distance in the Φ_h phase as demonstrated by the observed diffuse meridian reflection.

Supporting Table ST2. Structure Analysis of Chiral and Linear CTVs by XRD

Sample	T (℃)	Phase [a]	*a*, *b*, *c* (Å) [b]	d_{100}, d_{110}, d_{200}, d_{210}, d_{300}, d_{310}, d_{400}, d_{320}, d_{500}, d_{420}, d_{600}, d_{620}, d_{311}, d_{411} (Å) [c] d_{421}, d_{511}, d_{431}, d_{322}, d_{332}, d_{422}, d_{432}, d_{303}, d_{313}, d_{413}, d_{423}, d_{004}, d_{304}, d_{224} (Å) [d] d_{10}, d_{11}, d_{20}, d_{21} (Å) [e] d_{10}, d_{01}, d_{11}, d_{20}, d_{31}, d_{33}, d_{42} (Å) [f]
(3,4)dm8*G1-CTV 100% R	20	Φ_h^k	34.3, 34.3, 18.5	29.7, 17.2, 14.9, 11.2, 9.9, 8.2, 7.4, 6.8, 5.9, 5.6, 5.0, 4.1, 7.5, 6.1 [c] 5.4, 5.0, 4.7, 5.5, 4.9, 4.8, 4.3, 5.2, 4.9, 4.5, 4.2, 4.6, 4.2, 4.1 [d]
	75	Φ_h	33.2, 33.2, -	28.9, 16.6, 14.4, 10.9 [e]
(3,4)dm8*G1-CTV 100% S	20	Φ_h^k	34.3, 34.3, 18.5	29.7, 17.2, 14.9, 11.2, 9.9, 8.2, 7.4, 6.8, 5.9, 5.6, 5.0, 4.1, 7.5, 6.1 [c] 5.4, 5.0, 4.7, 5.5, 4.9, 4.8, 4.3, 5.2, 4.9, 4.5, 4.2, 4.6, 4.2, 4.1 [d]
	75	Φ_h	33.2, 33.2, -	28.9, 16.6, 14.4, 10.9 [e]
(3,4)dm8*G1-CTV 75% R + 25% S	20	Φ_h^k	34.3, 34.3, 18.5	29.7, 17.2, 14.9, 11.2, 9.9, 8.2, 7.4, 6.8, 5.9, 5.6, 5.0, 4.1, 7.5, 6.1 [c] 5.4, -, -, 5.5, 4.9, 4.8, 4.3, -, 4.9, 4.5, -, 4.6, 4.2, 4.1 [d]
	72	Φ_h	33.2, 33.2, -	28.9, 16.6, 14.4, 10.9 [e]
(3,4)dm8*G1-CTV 75% S + 25% R	20	Φ_h^k	34.3, 34.3, 18.5	29.7, 17.2, 14.9, 11.2, 9.9, 8.2, 7.4, 6.8, 5.9, 5.6, 5.0, 4.1, 7.5, 6.1 [c] 5.4, -, -, 5.5, 4.9, 4.8, 4.3, -, 4.9, 4.5, -, 4.6, 4.2, 4.1 [d]
	72	Φ_h	33.2, 33.2, -	28.9, 16.6, 14.4, 10.9 [e]
(3,4)dm8*G1-CTV 50% R + 50% S	20	Φ_h^k	34.3, 34.3, 18.5	29.7, 17.2, 14.9, 11.2, 9.9, 8.2, 7.4, 6.8, 5.9, 5.6, 5.0, 4.1, -, - [c] -, -, -, 5.5, -, 4.8, -, -, 4.9, 4.5, -, 4.6, 4.2, - [d]
	72	Φ_h	33.2, 33.2, -	28.9, 16.6, 14.4, 10.9 [e]
(3,4)dm8*G1-CTV racemic by synthesis	20	Φ_h^{io}	34.3, 34.3, -	29.7, 17.2, 14.9, 11.2, 9.9, 8.2, 7.4, 6.8, 5.9, 5.6, 5.0, 4.1, -, - [c] -, -, -, -, -, 4.8, -, -, -, 4.5, -, 4.6, 4.2, - [d]
	72	Φ_h	33.2, 33.2, -	28.9, 16.6, 14.4, 10.9 [e]
(3,4)12G1-CTV linear achiral chain	-20	Φ_{rec}^{io}	35.5, 30.8, -	35.5, 30.8, 23.3, 17.8, 11.1, 7.8, 7.7 [f]
	100	Φ_h	35.7, 35.7, -	30.9, 17.9, 15.5, - [e]
(3,4)8G1-CTV linear achiral chain	20	Φ_h^k	31.5, 31.5, 18.9	27.3, 15.6, 13.6, 10.3, 9.1, 7.6, 6.8, 6.3, 5.5, 5.2, 4.6, 3.8, -, 5.7 [c] 5.0, 4.7, 4.4, -, -, -, -, -, -, -, -, -, 4.7, 4.2, - [d]
	105	Φ_h	31.5, 31.5, -	27.3, 15.8, 13.6, 10.3 [e]

[a] Phase notation: Φ_h^k – columnar hexagonal crystalline phase; Φ_h^{io} – 2D columnar hexagonal phase with intra-columnar order; Φ_h – 2D columnar hexagonal phase without intra-columnar order; Φ_{rec}^{io} – 2D columnar rectangular phase with intra-columnar order; [b] Lattice parameters (with uncertainty of ~1%) calculated using $d_{hkl} = 1/(4(h^2 + k^2 + hk)/3a^2 + (l/c)^2)^{1/2}$ for hexagonal phase. [c, d] Experimental diffraction peak d-spacing for the Φ_h^k and Φ_h^{io} phase. [e] Experimental diffraction peak d-spacing for the Φ_h phase. [f] Experimental diffraction peak d-spacing for the Φ_{rec}^{io} phase.

Supporting Table ST3. Structural Analysis of Chiral and Linear CTVs by XRD and Experimental Density

n	T (℃)	Phase [a]	*a*, *b*, *c* (Å) [b]	D_{col} (Å) [c]	*t* (Å) [d]	ρ [e] (g/cm^3)	M_{wt} [f]	*n* [g]	μ [h]
(3,4)dm8*G1-CTV 100% R	20	Φ_h^k	34.3, 34.3, 18.5	34.3	4.6	1.04	2782.3	4	1
	75	Φ_h	33.2, 33.2, -	33.2	4.6			-	1
(3,4)dm8*G1-CTV 100% S	20	Φ_h^k	34.3, 34.3, 18.5	34.3	4.6	1.04	2782.3	4	1
	75	Φ_h	33.2, 33.2, -	33.2	4.6			-	1
(3,4)dm8*G1-CTV 75% R + 25% S	20	Φ_h^k	34.3, 34.3, 18.5	34.3	4.6	1.04	2782.3	4	1
	72	Φ_h	33.2, 33.2, -	33.2	4.6			-	1
(3,4)dm8*G1-CTV 75% S + 25% R	20	Φ_h^k	34.3, 34.3, 18.5	34.3	4.6	1.04	2782.3	4	1
	72	Φ_h	33.2, 33.2, -	33.2	4.6			-	1
(3,4)dm8*G1-CTV 50% R + 50% S	20	Φ_h^k	34.3, 34.3, 18.5	34.3	4.6	1.04	2782.3	4	1
	72	Φ_h	33.2, 33.2, -	33.2	4.6			-	1
(3,4)dm8*G1-CTV racemic by synthesis	20	Φ_h^{io}	34.3, 34.3, -	34.3	4.6	1.04	2782.3	-	1
	72	Φ_h	33.2, 33.2, -	33.2	4.6			-	1
(3,4)12G1-CTV linear achiral chain	-20	Φ_{rec}^{io}	35.5, 30.8, -	35.5	4.7	1.02	3119.0	-	1
	100	Φ_h	35.7, 35.7, -	35.7	4.7			-	1
(3,4)8G1-CTV linear achiral chain	20	Φ_h^k	31.5, 31.5, 18.9	31.5	4.7	1.05	2445.7	4	1
	105	Φ_h	31.5, 31.5, -	31.5	4.7			-	1

[a] Phase notation: Φ_h^k – columnar hexagonal crystalline phase; Φ_h^{io} – 2D columnar hexagonal phase with intra-columnar order; Φ_h – 2D columnar hexagonal phase without intra-columnar order; Φ_{rec}^{io} – 2D columnar rectangular phase with intra-columnar order; [b] Lattice parameters determined from fiber and powder X-ray diffractions. [c]Column diameter. [d]Stratum thickness calculated from the meriodional pattern. [e]Experimental density measured at 20 °C. [f]Molecular weight of the compound. [g]Average number of molecules per unit cell, calculated using $n = N_A \rho V_c / M_{wt}$, where $N_A = 6.022 \times 10^{23}$ mol^{-1} is the Avogadro's number, and V_c is the unit cell volume calculated from lattice parameters. [h]Average number of dendrimers forming the supramolecular column stratum, calculated using: $\mu = N_A \rho A t / 2M_{wt}$, where A is the unit cell area of *ab* plane, and *t* is the average strata thickness calculated from the meriodional pattern.

Supporting Tables ST2 and ST3 summarize the observed reflections in XRD patterns and structural analysis data.

7. Circular Dichroism (CD) and UV-Vis Absorption Experiments (CD/UV)

Circular dichroism (CD) and UV spectroscopy measurements were carried out in a Jasco J-720 Spectropolarimeter. The temperature was controlled by Peltier temperature controller (Jasco PTC-423) or with a Thermo Neslab RTE-111 refrigerated circulator digital temperature controller. Dodecane (99%, Acros) or 1-butanol (99.5%, spectrophotometric grade, Aldrich) were used as solvents. Spectra were recorded in 1-mm quartz cuvettes and corrected by subtracting the spectra of the pure solvent at the same temperature. A scan rate of 100 nm/min with a response time of 2 s and a bandwidth of 2 nm were used to measure the CD spectra, which were recorded between 320 and 180 nm.

Temperature-dependent CD/UV experiments with full spectra were performed by cooling 4.0×10^{-5} M dodecane solutions from 50 to 0 °C at a cooling rate of 30 °C per hour with measurement of full spectra at 1 °C intervals.

Thin film CD/UV experiments were carried on using the following procedure. A 2% w/v solution of the CTV dendrimer in chloroform was prepared by dissolving 5 mg of sample in 250 μL of solvent. The solution was spin-coated on a round quartz plate at 2500 rpm for 6 s and 7000 rpm for 30 s, using a Chemat Technology Spin Coater KW-4A. CD/UV spectra of thin films were recorded using the same parameters as those used for solution experiments, and the spectra were corrected by subtracting spectra of the quartz plate recorded before spin-coating.

Data of single-wavelength cooling experiments were recorded by cooling 4.0×10^{-5} M (or 8.0×10^{-5} M) *n*-butanol solutions of the desired sample at 30 °C per hour and measuring the CD/UV response at 206 nm at 0.1 °C intervals. The UV data were then rescaled between 0 and 1 to give the degree of aggregation ϕ using the following equation:

$$\phi(T) = \frac{A(T) - A_m}{A_a - A_m}$$

where $A(T)$ is the UV absorbance at 206 nm at temperature T, A_m is the absorbance at 206 nm in the molecularly dissolved state at high temperature and A_a is the absorbance at 206 nm in the aggregated state at low temperature. The mechanism of helical supramolecular polymerization was determined to be a cooperative nucleation-elongation mechanism from the curve profile obtained for $\phi(T)$, according to the method reported by Meijer and co-workers.[9]

Calculations of the elongation temperature Te and the enthalpy for supramolecular polymerization he were performed by fitting of the experimental data with the elongation equation:[10]

$$\Phi = \Phi_{SAT}\left[1 - exp\left(-\frac{h_e}{RT_e^2}(T - T_e)\right)\right]$$

where ϕ is the degree of aggregation, ϕ_{SAT} is the saturation level of the data, T is the temperature, T_e is the elongation temperature, h_e is the molar enthalpy for supramolecular polymerization and R is the gas constant.

The degree of aggregation and calculations performed on the UV data at 206 nm obtained from 4.0×10^{-5} M (total concentration) *n*-butanol solutions of the *R*, *S*, *"racemic by mixing"*, and *"racemic by synthesis"* samples are given in Supporting Figure SF4. As discussed in the main text of the article, due to deracemization in the *"racemic by mixing"* sample a solution containing 4.0×10^{-5} M of each enantiomer (*i.e.* a total concentration of 8.0×10^{-5} M) should be considered for direct comparison with the other samples.

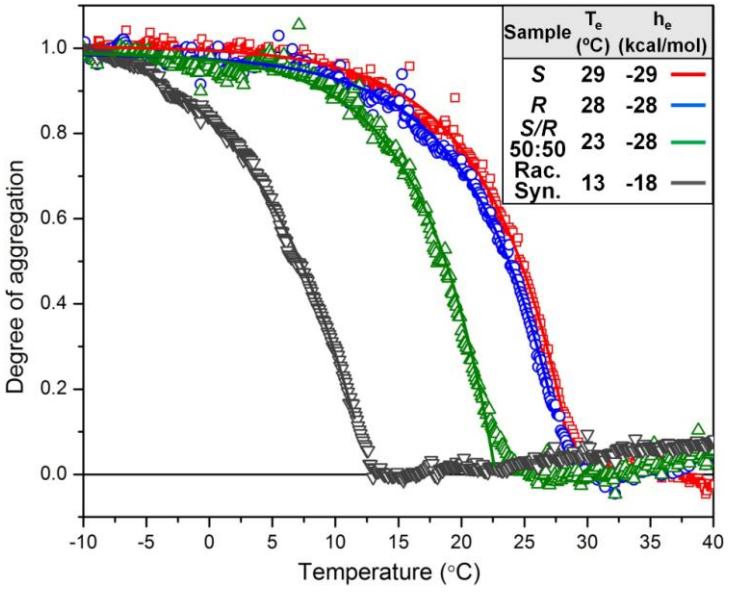

Supporting Figure SF4. Degree of aggregation (from UV absorption at 206 nm of 4.0×10^{-5} M solutions in *n*-butanol) collected upon cooling of *n*-butanol solutions from 50 °C to -10 °C, and fitting with the cooperative elongation model (solid lines).

The racemic and achiral dendronized CTV showed no Cotton effect in CD measurements upon cooling (see Supporting Figure SF5 for the comparison with spectrum obtained from chiral analog). The spectra are collected at 0 °C in a dodecane solution with concentration of 4.0×10^{-5} M. As elucidated in the main text, the columns from racemic or achiral samples are helical and non-racemic, but exist in a equal ratio of right and left handed conformations.

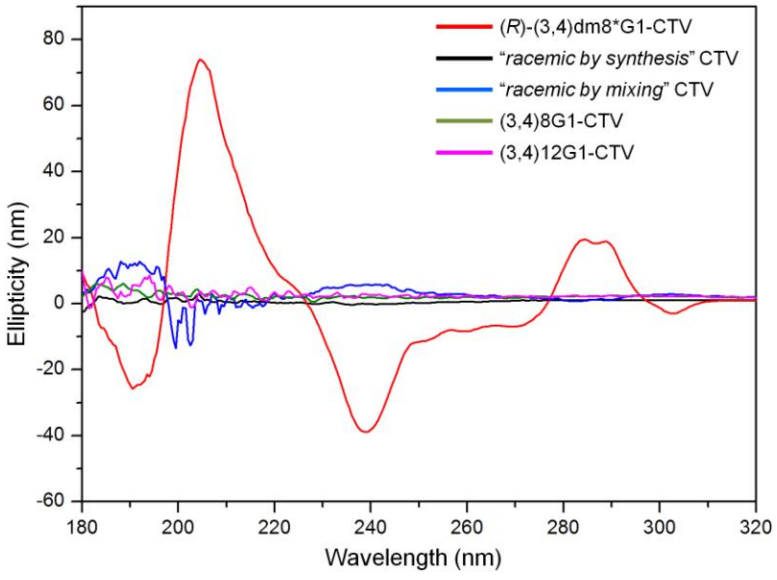

Supporting Figure SF5. Comparison of CD spectra between chiral (*R*)-(3,4)dm8*G1-CTV, "*racemic by synthesis*" CTV, "*racemic by mixing*" CTV, achiral (3,4)8G1-CTV, and achiral (3,4)12G1-CTV. Data collected at 0 ℃ with concentration of 4.0×10^{-5} M in dodecane.

The spectra of *(S)*-(3,4)dm8*G1-CTV in dodecane and in *n*-butanol solutions were compared to control that the self-assembled structures formed in these solvents are the same (Supporting Figure SF6). Identical spectra were obtained, which allows us to compare experiments performed in both solvents.

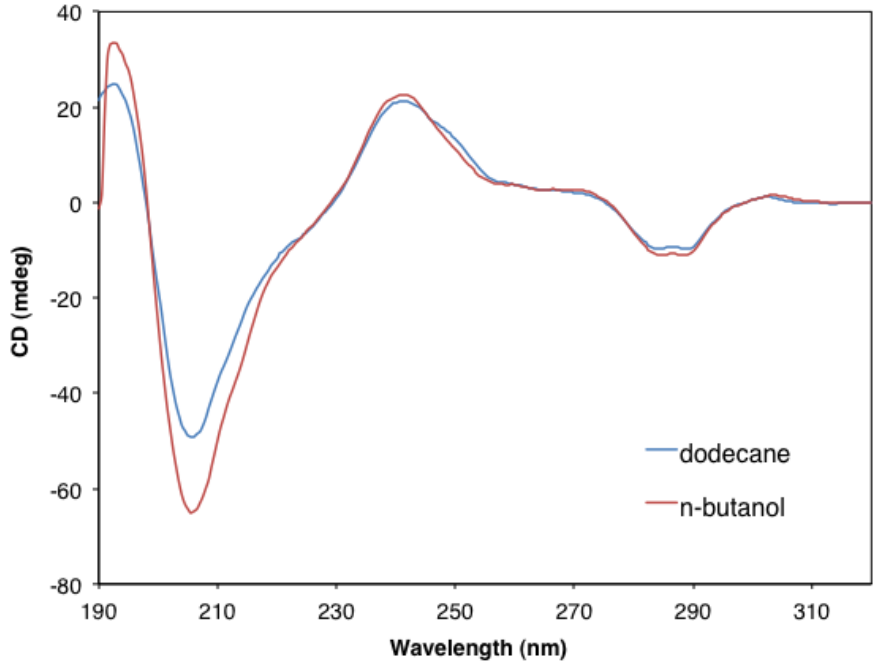

Supporting Figure SF6. Comparison of the CD spectra of *(S)*-(3,4)dm8*G1-CTV in dodecane and in *n*-butanol (4.0×10^{-5} M solutions, 0 ℃).

A "temperature-hold experiment" was performed to determine whether cooling or heating data reflect the thermodynamic behavior of the system and which part of the data is more affected by kinetic effects. A 8.0×10^{-5} M solution of *(S)*-(3,4)dm8*G1-CTV was cooled down from 50 ℃ to 0 ℃ and then heated up

from 0 to 25 °C (the center temperature of the hysteresis cycle) while recording the CD signal at 240 nm. The temperature was then held at 25 °C and CD changes with time monitored at 240 nm. Slow decay of the CD signal upon temperature holding at 25 °C demonstrates that the self-assembled state is not thermodynamically stable at this temperature (Supporting Figure SF7).

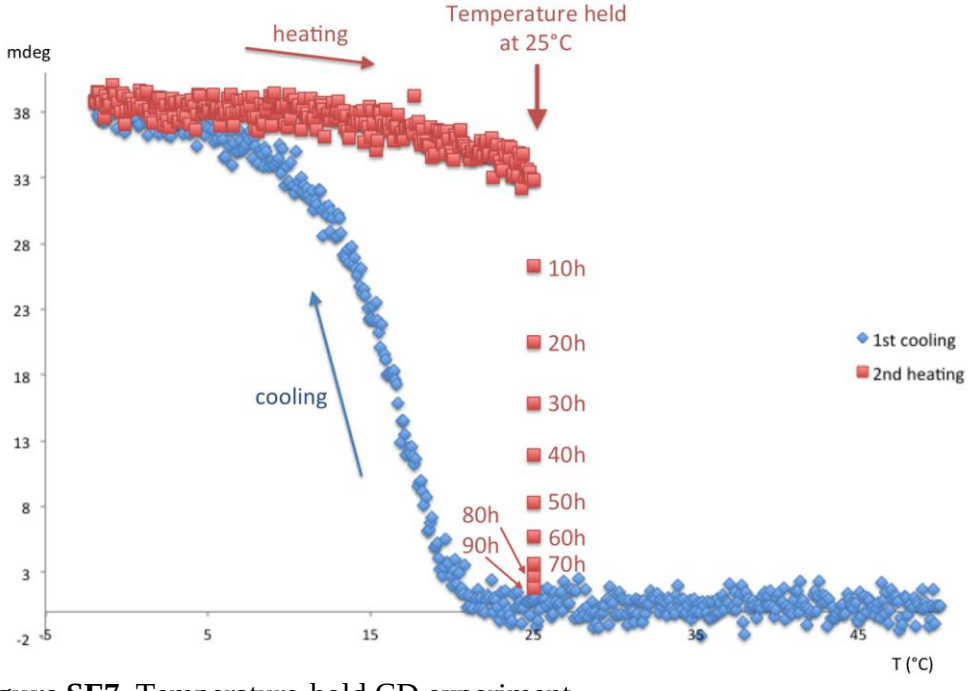

Supporting Figure SF7. Temperature-hold CD experiment.

The entropy of the helical supramolecular polymerization was calculated from a Van't Hoff plot (Supporting Figure SF8). The elongation temperature were determined for *(S)*-(3,4)dm8*G1-CTV in *n*-butanol at different concentrations, and the results were linearly fitted with the following equation:

$$R * \ln C = \Delta H_e \times \frac{1}{T_e} - \Delta S_e$$

where R (J.mol^{-1}.K^{-1}) is the gas constant, C is the concentration, ΔH_e (J.mol^{-1}) is the enthalpy, T_e (K) is the elongation temperature and ΔS_e (J.mol^{-1}.K^{-1}) is the entropy.

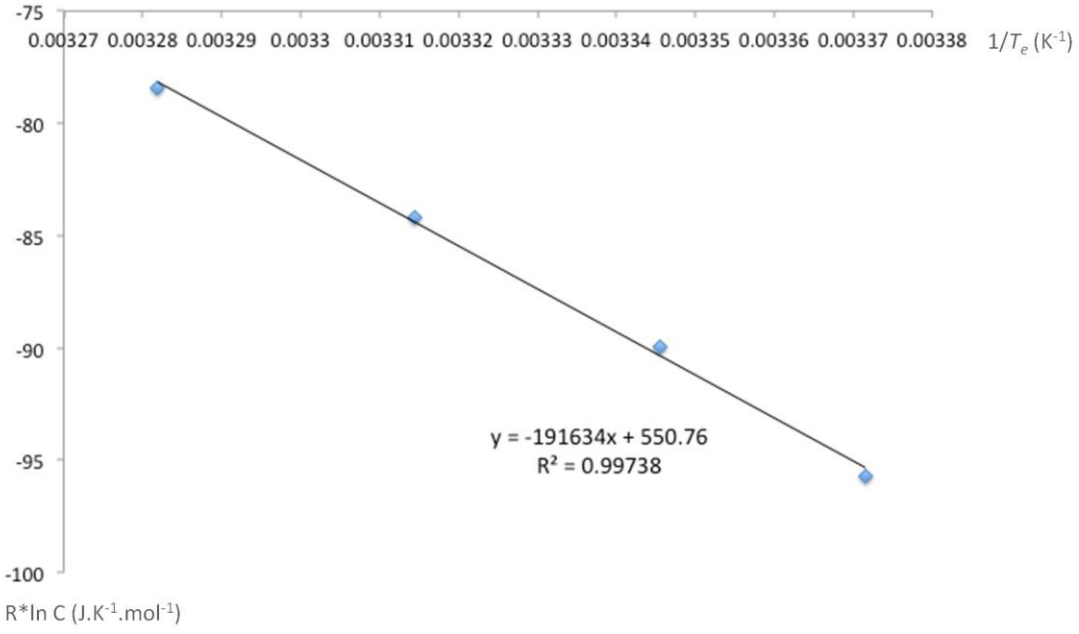

Supporting Figure SF8. Van't Hoff plot for *(S)*-(3,4)dm8*G1-CTV in *n*-butanol.

For the majority-rules experiment, mixtures of *(R)* and *(S)* enantiomers of (3,4)dm8*G1-CTV in different proportions (respectively 0%, 10%, 20%, 30%, 40%, 50%, 60%, 70%, 80%, 90%, 100% of *(R)* enantiomer) were prepared as 4.0×10^{-5} M solutions (total concentration) in dodecane. The solutions were cooled from 50 °C to 0 °C at 30 °C per hour, and their CD spectra were then recorded at 0 °C. The net helicity was calculated by dividing the ellipticity of each sample by the ellipticity measured for the pure enantiomers at 289 nm.

At this point we would also like to comment on the accuracy of the method used to determine the enthalpy h_e. The parameters T_e and h_e are both obtained from the experimental UV data at a given wavelength recorded upon cooling, by fitting with the elongation equation eq 1. After numerous calculations from data collected at various wavelengths, we found out that the fitting results - especially for h_e - are dependent on the wavelength chosen for calculation. This dependence can be rationalized if we consider the possibility that changes in the UV spectra may results from various phenomena, including but not limited to helical supramolecular polymerization. Formation of multiple supramolecular structures may occur simultaneously, for example formation of supramolecular dimers and short disordered stacks. While the CD and UV spectra obtained are characteristic of a helical supramolecular polymerization process, minor contributions from other structures cannot be excluded. These minor contributions introduce errors in the fitting calculations, therefore the results for T_e and h_e cannot be obtained with absolute accuracy, and minor differences between similar systems might not be detected.

8. Variable Temperature ^{13}C CP-MAS NMR studies of (3,4)8G1-CTV

Variable temperature ^{13}C CP-MAS measurements of (3,4)8G1-CTV similar to those of the "*racemic by synthesis*" (3,4)dm8*G1-CTV shown in the manuscript, in order to analyze the dynamic behavior of the CTV core in the system with linear side chains.

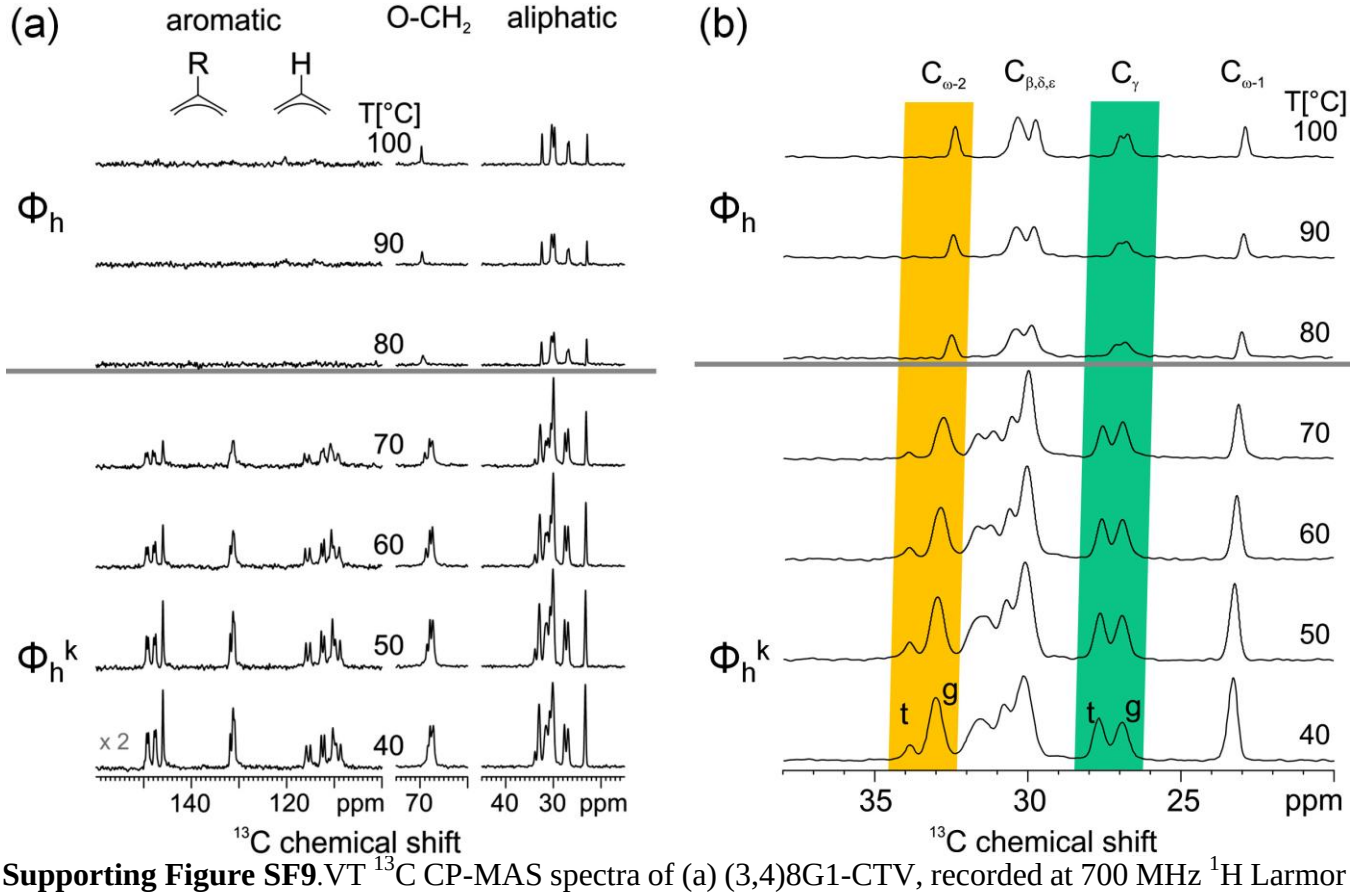

Supporting Figure SF9.VT ^{13}C CP-MAS spectra of (a) (3,4)8G1-CTV, recorded at 700 MHz ^{1}H Larmor and 25 kHz MAS spinning frequency. As indicated different spectral regions are plotted on different intensity scales. (b) The spectra of aliphatic side chains of (3,4)8G1-CTV (zoom from (a)).

The observed dynamic behavior of (3,4)8G1-CTV is very similar to that of the "*racemic by synthesis*" CTV. As described in the manuscript, CP-MAS signals are reduced by motional averaging of the hetero-nuclear dipolar coupling. Remarkably this signal reduction averages already in the hexagonal meso-phase the signals of the central CTV core to zero, while the signals of the aliphatic side chains are reduced in the meso phase, but do not vanish over the whole temperature range accessible to our NMR probes. Moreover, the reappearance of signals originating from ^{13}C sites of CTV core at higher temperatures, as it could be observed in the "*racemic by synthesis*" sample, could not be observed in the achiral linear substituted CTV sample. However, it is worth having a closer look to the NMR signals of the alphatic side chains in the crystalline hexagonal phase.

In the hexagonal meso-phase at temperatures above 70°C, the different ^{13}C signals can be relatively straight forward be assigned to different ^{13}C sites along the octane chain. It should be noted, that only the ^{13}C sites in γ position to the oxygen bridging to the phenyl ring, show a tendency toward conformational splitting of the signal, indicating the presence of octane chains with minor differences in the local

conformation of the γ position. For all other sites, the molecular mobility is sufficient to achieve complete conformational averaging. In the crystalline hexagonal phase, however, only the signal of the methyl site at 14 ppm (ω position, not shown in the spectra) and the signal of the methylene group next to it (ω-1 position) observed around ~23 ppm are not split or broadened due to a heterogeneous distribution of conformations along the octane chain. In fact the signals of the γ and the ω-2 position can be easily analyzed, providing a gauche/trans ratio of 7-8 for the ω-2 position, while the gauche/trans ration for the γ site is close to 1. This nicely confirms the increasing probability finding gauche conformations towards the chains ends of the octane chains obtained from x-ray. Moreover, it should be pointed out that the gauche/trans ratio is increasing for both sites with increasing temperature.

9. Comparison of Column Packing Models with Different Side Chain Orientation

If the branched alkyl groups were all straight and tilted to the column as shown in Supporting Figure SF10a (model 2 from Figure 5f in the main text), the columns would have to exhibit strictly up-down alternation (antiparallel) to ensure effective packing between the columns. Therefore it would require two columns per unit cell and thus reduce the 3D hexagonal symmetry to orthorhombic or monoclinic. This requirement does not hold for the bent-branch pine-tree structure generated by the "hat-shaped" dendronized CTV (Supporting Figure SF10b, (model 3 from Figure 5i in the main text)) since the alkyl chain packing in between adjacent columns is not affected by the column orientation.

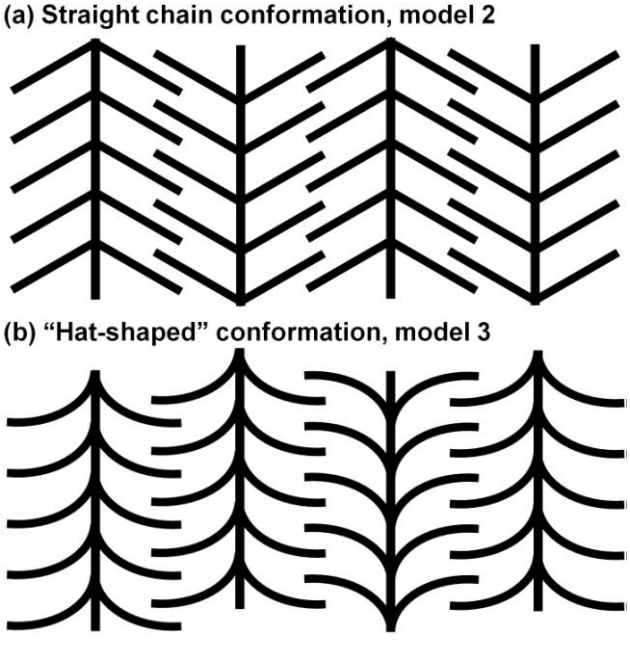

Supporting Figure SF10. Column packing models for: (a) tilted alkyl groups of the pine-tree columnar structure (model 2 from Figure 5f), and (b) bent-branch pine-tree structure produced by "hat-shaped" dendronized CTV (model 3 in Figure 5i). In (a), the 3D hexagonal symmetry would reduce to orthorhombic or monoclinic due to the requirement of strictly up-down two columns per unit cell.

10. References for the Supporting Information

(1) Percec, V.; Sun, H.-J.; Leowanawat, P.; Peterca, M.; Graf, R.; Spiess, H. W.; Zeng, X.; Ungar, G.; Heiney, P. A. *J. Am. Chem. Soc.* **2013**, *135*, 4129-4148.

(2) Scott, J. L.; MacFarlane, D. R.; Raston, C. L.; Teoh, C. M. *Green Chem.* **2000**, *2*, 123-126.

(3) Trzaska, S. T.; Hsu, H.-F.; Swager, T. M. *J. Am. Chem. Soc.* **1999**, *121*, 4518-4519.

(4) (a) Peterca, M.; Percec, V.; Imam, M. R.; Leowanawat, P.; Morimitsu, K.; Heiney, P. A. *J. Am. Chem. Soc.* **2008**, *130*, 14840-14852. (b) Percec, V.; Imam, M. R.; Peterca, M.; Wilson, D. A.; Heiney, P. A. *J. Am. Chem. Soc.* **2009**, *131*, 1294-1304.

(5) Percec, V.; Rudick, J. G.; Peterca, M.; Wagner, M.; Obata, M.; Mitchell, C. M.; Cho, W.-D.; Balagurusamy, V. S. K.; Heiney, P. A. *J. Am. Chem. Soc.* **2005**, *127*, 15257-15264.

(6) (a) Lindsey, A. S. *J. Chem. Soc.* **1965**, 1685-1692. (b) Hyatt, J. A. *J. Org. Chem.* **1978**, *43*, 1808-1811.

(7) Jacques, J.; Collet, A.; Wilen, S. H. *Enantiomers, Racemates and Resolutions*; Krieger Pub. Co.: Malabar, Fl, 1991.

(8) Rosen, B. M.; Peterca, M.; Morimitsu, K.; Dulcey, A. E.; Leowanawat, P.; Resmerita, A.-M.; Imam, M. R.; Percec, V. *J. Am. Chem. Soc.* **2011**, *133*, 5135-5151.

(9) Smulders, M. M. J.; Nieuwenhuizen, M. M. L.; de Greef, T. F. A.; van der Schoot, P.; Schenning, A. P. H. J.; Meijer, E. W. *Chem. Eur. J.* **2010**, *16*, 362-367.

(10) Jonkheijm, P.; van der Schoot, P.; Schenning, A. P. H. J.; Meijer, E. W. *Science* **2006**, *313*, 80-83.